Bachelor's Thesis

Setup of a Laser System for a Magneto-Optical Trap of Lithium

Submitted to the University of Stuttgart by

Utzuri Ursula Högl Vidal

July 25, 2024

5. Physikalisches Institut

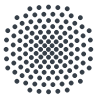

University of Stuttgart
Germany

Examiner:

Prof. Dr. Tilman Pfau

Declaration of Ownership

I hereby declare that this thesis is my own work and I did not use the work of others except when explicitly stated. All pages and ideas taken from others have been clearly indicated as such. The printed and electronic versions of this thesis are identical. Neither this thesis as a whole nor significant parts of it have been a part of another exam. I also declare that I have not made use of any AI-assisted writing tools.

Stuttgart, 25.07.2024

Utzuri Ursula Högl Vidal

Abstract

This work presents the results of the setup and characterization of a laser system used for the cooling of lithium atoms via gray molasses cooling. The laser was initially set up, tuned to the correct wavelength and its beam profile was improved. Next, Doppler-limited and Doppler-free spectroscopy was conducted. A second laser, applied in the Zeeman slower and Magneto-Optical trap of the experiment, was also used for conducting experiments, such as spectroscopy. Finally, the frequency of both lasers was successfully locked using the Pound-Drever-Hall method.

Zusammenfassung

In dieser Arbeit werden die Ergebnisse des Aufbaus und der Charakterisierung eines Lasersystems vorgestellt, das für die Kühlung von Lithiumatomen mittels grauer Molasse verwendet wird. Der Laser wurde zunächst eingerichtet, auf die richtige Wellenlänge gebracht und sein Strahlprofil verbessert. Anschließend wurde eine reguläre und Dopplerfreie Spektroskopie durchgeführt. Ein zweiter Laser, der im Experiment später für den Zeeman-Slower und für die Magneto-Optische Falle eingesetzt wird, wurde ebenfalls für Spektroskopie Messungen verwendet. Schließlich wurde die Frequenz beider Laser mit Hilfe der Pound-Drever-Hall-Methode erfolgreich stabilisiert.

Contents

1 Introduction

In recent years laser cooling and trapping techniques have made rapid progress in the fields of atomic and molecular physics. These improvements enabled the development of imaging techniques, such as quantum gas microscopy [1] [2] and charged particle detection [3]. Typically, well understood and comparatively undemanding atomic species like rubidium tend to be used in experiments.

However, more exotic species may possess interesting properties. One such atomic species is lithium, which is the lightest of all alkali metals. Elements of this group only have one outer electron, giving them a hydrogen-like energy structure that simplifies laser cooling. In our experiment we use the fermionic ^{6}Li, which is one of two stable isotopes of lithium besides the bosonic ^{7}Li. With this isotope a variety of different quantum effects can be investigated, one of them is the creation of a Fermi-sea. Another interesting application of lithium is its usage in atom-ion-scattering events [4]. So far the s-wave-scattering (or quantum) regime has only been reached for atom-atom collisions. Lithium's low mass makes it a prime candidate for achieving this milestone even in atom-ion systems [5].

One of the main goals of the ion microscope is to realize an ultra-cold dense atomic gas of ^{6}Li atoms. With this cloud, the aforementioned quantum effects can be investigated and detected with a spatial resolution of 200 nm [6]. As the ion microscope is currently only operated with rubidium, the addition of lithium will enable a dual species operation, which allows for the research of phenomena such as impurity physics. The first step towards implementing lithium in the already existing experiment is to set up and frequency lock the required cooling lasers. To end up with an ultra cold cloud of lithium, the atoms have to be decelerated with a Zeeman slower, trapped with a Magneto-Optical Trap (MOT) and further cooled down via the gray molasses technique. This can be achieved with two different lasers driving the D1 and D2 transitions, respectively. In this thesis, the setup and characterization of the D1 laser is performed. Furthermore, spectroscopy measurements were conducted with both the D1 and D2 lasers. This is done in order to implement frequency stabilization using the Pound-Drever-Hall technique, allowing for effective cooling and trapping of lithium for conducting the aforementioned experiments.

2 Ion Microscope

An ion microscope provides the possibility to detect charged particles with high resolution beyond the optical diffraction limit for standard optical imaging. Among many other applications, this also allows for the spatially resolved investigation of ultracold atomic samples and quantum gases [6]. Furthermore, the high temporal resolution of multi-channel plate detector (MCP) enables time-resolved observation of dynamic processes. The current experiment is conducted with rubidium as a first step to set up the machine [7] [8].

The experimental sequence of the ion microscope can be divided into two categories. The first part of the experiment involves creating an atomic beam and then slowing down and trapping the atoms and finally to prepare a cold atomic cloud below the ion microscope detector. In the second part of the experimental cycle, the actual experiment takes place, which is followed by the imaging process using the ion microscope.

To generate an atomic beam, an effusive oven is used. Due to the high ejection velocities, the atoms must then be slowed down in order to trap them in the Magneto Optical Trap (MOT) and undergo additional subsequent cooling steps before further investigation. The first step is to slow them through the Zeeman slower, which uses a laser (Light Amplification by Stimulated Emission of Radiation) that opposes the direction of the atomic beam and a magnetic field gradient. This slows the atoms sufficiently down to load them into a Magneto Optical Trap (MOT), where three pairs of counterpropagating laser beams and two coils in an anti-Helmholtz configuration, which create a magnetic field, trap the atoms. The next trapping step compresses the MOT by increasing the magnetic field gradient to achieve higher densities and better confinement of the atoms. The next cooling stage is bright optical molasses, similar to a MOT but without the anti-Helmholtz coils, creating a velocity-dependent force that further cools the atoms without trapping them.

After the atoms have been cooled down, they need to be transported to the science chamber. This can be achieved with an optical dipole trap. For a red detuned laser like in this experiment, the atoms are attracted to the intensity maxima of the beam. The dipole trap allows the trapped atoms to be spatially moved by mechanically moving the focus of the beam by using an optical lens on an air-bearing translation stage. In the second part of the experimental sequence, the actual experiment is carried out, which involves typically the creation of a Rydberg atom

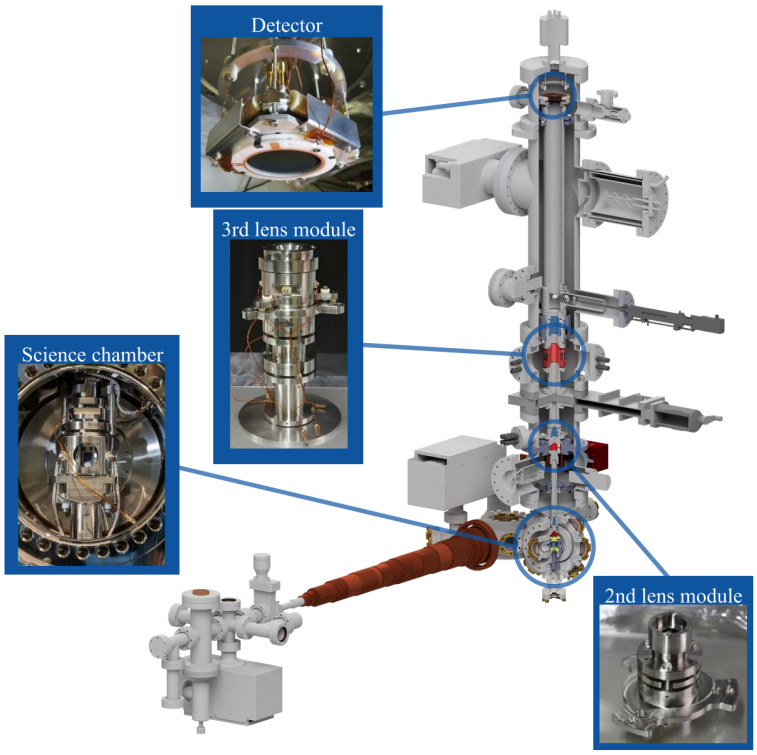

Fig. 1: Schematic diagram of the ion microscope. The atoms start their journey to the science chamber from the box on the bottom left. This is the oven, then they pass through the Zeeman slower, which is painted brown. After that, the cylinder with several windows is the MOT. Next is the science chamber. This is where the particles collide and are then transported through the three electrostatic lenses to the detector at the top of the microscope. Figure taken from [9].

using a two-photon excitation scheme or the direct creation of an ion via a two-photon ionization process. To be able to detect neutral Rydbgerg atoms with the ion microscope, the Rydberg atom is field ionized before the imaging process. Six field electrodes in the science chamber allow the compensation of the electric fields during the experiment well enough so that there is no need for a radio frequency field for trapping the ion. This advantage helps achieve lower temperatures. The particles involved in the experiment are then transported to the detector plate passing three electrostatic lenses with varying voltages. Depending on the applied voltage, magnifications between 200 and 1500 can be achieved with a resolution of up to 200 nm [10].

With this setup many different experiments can be conducted. One of them is to examine the interaction between an ion and a Rydberg atom. Out of this measurements the location of the Rydberg core can be measured. Also the s-wave scattering in the collision between an ion and neutral atom can be achieved [11] [7] [8]. Up to date this regime could only be reached between neutral atoms. However, collisions between an ion and a ground state atom have not reached the s-wave scattering regime yet, although some groups have observed charged-neutral collisions close to it [12].

To reach the s-wave scattering between a charged and a neutral atom atomic species with very low mass are advantageous. For such an experiments is rubidium too heavy, but with lithium the s-wave scattering regime should be reachable [5]. This is why the ion microscope will be extended to be used with two species, the already in use rubidium and the one with which the s-wave scattering can be reached, lithium. This element has a fermionic character, and thus can be used to do research on fermionic specific properties like Fermi-sea interactions. After the implementation of the elements needed for the ion microscope to work with both rubidium and lithium, the interaction between them both can also be investigated.

3 Theoretical Background

3.1 Characteristics of Lithium

In the ion microscope, lithium will be one of the two elements used, besides rubidium. As an alkali metal, it has only one valence electron, which results in a hydrogen-like level structure ideal for laser cooling. Lithium is the lightest alkali metal. In the experiment the s-wave scattering regime of an ion and a neutral atom will be investigated in the future and this regime is easier to achieve the lower the mass of investigated atoms is. To reach this zone, the atoms have to be cooled down to very low temperatures via laser cooling and other techniques like evaporative cooling. Ideally even lighter atoms like hydrogen or helium should be used, but it is complicated to reach the wavelengths that these elements need for laser cooling. Due to these reasons lithium is the element of choice; it has one controllable valence electron, a very low mass for easier access to the s-wave scattering regime and the wavelengths needed for laser cooling are available in currently existing laser systems.

In order to work with lithium, knowing its chemical and physical properties is important. Lithium has two stable isotopes that differ in their number of neutrons, ^{6}Li has three neutrons and ^{7}Li has four. Neutrons are particles with a spin value of 1/2. As the two isotopes have different nuclear spin values, they obey different quantum statistic:; the isotope ^{6}Li is a fermion and ^{7}Li a boson. They also differ in their natural abundance, ^{6}Li makes up only 7.59% of all stable lithium, the rest is made up from ^{7}Li (92.41%). They also differ in their masses as ^{6}Li has a lower mass (6.015 u) than ^{7}Li (7.016 u) [13]. Although both isotopes can theoretically be used for scattering purposes, the experiment only uses ^{6}Li. This is due to the fermionic nature of ^{6}Li, which is interesting for future research like the investigation of a lithium Fermi-sea. The fundamental properties of both isotopes of lithium can be seen in Table 1.

To generate single atoms from a lithium bulk the element is heated up until enough atoms change from the solid phase to the gaseous phase. These atoms are later going to create an atomic beam, hence a high enough vapor pressure is needed. Following these reasons lithium is heated up to a temperature of about 400 °C. For constructing the oven, where some experiments such as spectroscopy are conducted, multiple considerations have to be taken into account. As the lithium has to be heated up to be in the gas phase, it has to be considered that these atoms react with quartz glass for temperatures higher than 300 °C. This is why

Tab. 1: Fundamental physical properties and their symbols for the two isotopes of lithium, ^{6}Li and ^{7}Li [13].

Property	**Symbol**	**Value (^{6}Li)**	**Value (^{7}Li)**
Atomic Number	Z	3	3
Nucleons	$Z+N$	6	7
Natural Abundance	η	7.59 %	92.41 %
Nuclear Lifetime	τ_n	stable	stable
Atomic Mass	m	6.0151214 u $9.988\,341\,4 \times 10^{-27}$ kg	7.0160040 u $1.165\,883\,5 \times 10^{-26}$ kg
Total Electronic Spin	S	1/2	1/2
Total Nuclear Spin	I	1	3/2
Electronic Configuration		[He]2s^1	[He]2s^1

the windows of the oven cannot be made out of this material. Normally a buffer gas is used in the oven so that the high temperature lithium atoms remain in the middle of the chamber. The lithium atoms that fly further away do not have such high temperatures anymore, due to the collisions with the buffer gas. Using this technique it can be avoided that high temperature lithium expands throughout the oven allowing the usage of glass windows.

3.1.1 Electronic Structure of the D Lines in ^{6}Li

Alkali atoms have a favorable hydrogen-like level structure which makes them particularly attractive for laser cooling. As a result, many research projects all around the world work with them, therefore they are a well-studied atomic species. They are usually cooled down with lasers that drive the transition from the ground state ($n^2S_{1/2}$) to the lowest excited state ($n^2P_{1/2}$) for the D1 line or the second-lowest excited state ($n^2P_{3/2}$) for the D2 line.

The D line can be understood as a single transition between the ground state and the first electronic excited state according to the central field approximation, where the valence electron is treated as independent of the nucleus and the closed electronic shell and the nucleus are understood as a spherically symmetric electric field. However, spectroscopy shows that this transition is composed of two different electronic transitions. This is because the excited state is split into two energy levels, which can be described by the fine structure theory. This can be seen in the middle lines of the energy splitting in Figure 2.

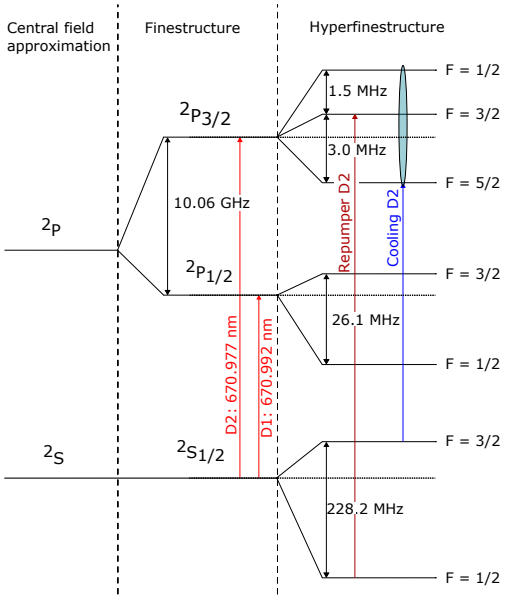

Fig. 2: Level scheme of the isotope ^{6}Li. On the left side the energy levels follow the central field approximation. In the central part the energy levels are represented via the fine structure theory, the levels are named after their $\hat{J}$ quantum number (total angular electric momentum). On the right side the energy levels are represented according to the hyperfine structure, the levels are named after their $\hat{F}$ quantum number (total atomic angular momentum). The light red lines represent the transitions named D1 and D2. The dark red line represents the transition used to repump the atoms from the lowest ground state $2^2S_{1/2}$ to the excited state $2^2P_{3/2}$. The cooling transitions used are pictured in light blue. The distance in frequency between the states is written in black [13].

The splitting of the D line into the D1 and the D2 line arises from the interaction between the spin of the valence electron and the angular momentum produced via its orbital motion around the nucleus. These two momenta generate two different interacting magnetic dipole moments that result in a splitting of the electronic energy levels. This effect is known as spin-orbit coupling and is included in the fine structure of the atoms. The resulting energy levels are represented in the central three lines of the energy diagram in Figure 2. The D1 and D2 lines have a separation of 10.0528 GHz as their wavelengths are 670.992 nm and 670.997 nm, respectively [13]. To describe the shift between the energy levels, the quantum operator $\hat{J}$ is introduced. It represents the sum of the orbital angular momentum $\hat{L}$ and the spin $\hat{S}$ of the valence electron ($\hat{J} = \hat{L} + \hat{S}$) and is named electronic angular momentum. The spectroscopy measurements of lithium show that the

Tab. 2: Optical properties of the D_1 and D_2 lines of ^{6}Li [13].

Property	**Symbol**	**Value for D1**	**Value for D2**
Wavelength (vacuum)	λ	670.992 421 nm	670.977 338 nm
Frequency	ν	446.789 634 THz	446.799 677 THz
Natural Linewidth	Γ	36.898 $\times 10^6$ s^{-1} 5.8724 MHz	36.898 $\times 10^6$ s^{-1} 5.8724 MHz

energy levels of the ground and the two lower excited states split even further into more energy levels. This is known as the hyperfine splitting, which emerges from the fact that the atomic nucleus is not spherically symmetric. It causes the appearance of a magnetic dipole and an electric quadropole moment of the nucleus, whose interactions with the electron lead to a further splitting of the energy levels. These interactions can be summed up as the hyperfine splitting and can be represented via the quantum operator $\hat{F}$ named total atomic angular momentum operator. It is composed of the sum of the total nuclear angular momentum $\hat{I}$ and the total electronic angular momentum $\hat{J}$; $\hat{F} = \hat{I} + \hat{J}$. This effect splits the different energy levels in various spectral lines that can be seen in the most right part of the energy diagram in Figure 2. All the main characteristics of the D1 and D2 line of lithium can be seen in Table 2.
The hyperfine levels of lithium are ordered corresponding to their energies following the equation [13]

$$\Delta E_{\mathrm{HF}} = \frac{1}{2} A\, C + \frac{3}{8} B\, \frac{C(C+1)}{I\,(2I-1)\,J\,(2J-1)}, \tag{3.1}$$

where A and B are the magnetic dipole and the electric quadrupole hyperfine constants, respectively and $C = F(F+1) - J(J+1) - I(I+1)$. The values of the constants for lithium are: $A_{2^2S_{1/2}} = 152.136\ 840\ 7$ MHz; $A_{2^2P_{1/2}} = 17.386$ MHz; $A_{2^2P_{3/2}} = $ -1.155 MHz and $B_{2^2P_{3/2}} = $ -0.10 MHz.

3.2 Diode Lasers

Diodes are electronic devices that can be used as a switch for current as they allow or forbid the passage of electrons through it. They are made out of a semiconductor material. In semiconductors the valence band and the conduction band are not overlapping, but energetically close to each other, so that with a small amount of energy input, typically thermal, the material becomes conductive. To favor the flow of electrons through the material, it is advantageous to have as many

free charge carriers as possible. To add more electrons and holes to the system the semiconductor can be doped with elements that possess either more valence electrons or more holes than the semiconductor element; for example if the semiconductor material is silicon (four valence electrons) the addition of boron (three valence electrons) produces an increase in the number of free holes, or the addition of phosphorus (five valence electrons) increases the number of free electrons. These two ways of doping a semiconductor can be used to produce a diode by creating an excess of electrons on one side of the semiconductor and an excess of holes on the other side of the semiconductor. As these two doped sides are close together, the electrons and holes recombine in their contact area. This causes electrons to accumulate in the p-doped zone and holes to accumulate in the n-doped zone, creating an uneven charge distribution that counteracts and eventually stops the drift of the carriers, creating an electric field in the area where the carriers have recombined. The recombination process creates a region where there are no free carriers, meaning that the semiconductor is an insulator in this region. To allow current to flow, an external electric field can be applied to counteract the effect of the internal electric field. As soon as the external electric field is greater than the internal one, the charge carriers of the depletion zone leave it. Then there is a sufficient amount of free charge carriers, which means that the insulating regime disappears and current can flow through. If the external electric field is applied in the same direction as the internal electric field, the insulating region becomes larger and no current can flow.
When the electrons and the holes in direct semiconductors recombine, they release energy in the form of photons. These photons can be used to produce a light source such as how it is done in Light Emitting Diodes (LEDs). This can also be used to construct a laser.

The building blocks of a laser are an active medium, an optical cavity and a pump. The first step in producing a coherent light beam in a laser is achieving a population inversion in the active medium. This means that there are more electrons in the excited states than in the ground state. These excited state atoms can generate photons by decaying from the excited to the ground state. To achieve population inversion, energy must be pumped into the active medium. This can be achieved electrically (e.g. by electric current) or optically (light irradiation). The pump process must take place at a different transition than the stimulated emission to be able to achieve population inversion. With this configuration, there is already light emission in the active medium, but the photons are produced through spontaneous emission, so the light is incoherent. To achieve coherent light and thus creating a laser, stimulated creation of photons is needed. This problem can be solved by constructing a resonator. It is normally made out of two mirrors with

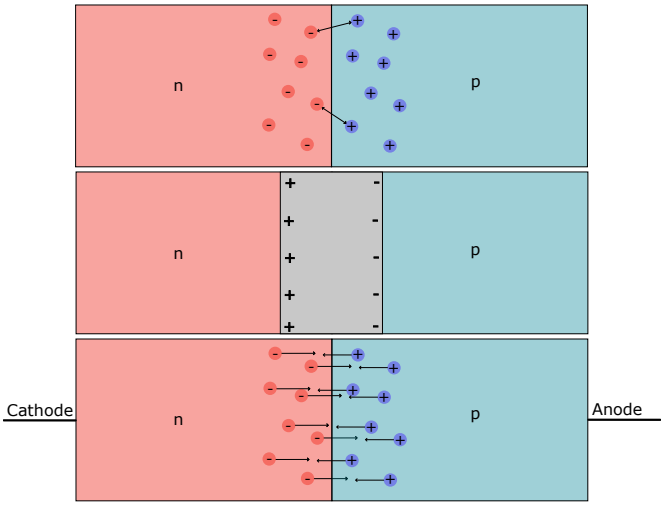

Fig. 3: Graph of different stages in a working diode. In the upper picture the n- and p-doped sites of the semiconductor and its free charge carriers can be seen. These charge carriers recombine and due to this recombination and the electric field caused by its motion a blockade arises, this can be seen in gray. The pluses and minuses represent the electric field. In the bottom picture current is being applied to the diode, from the cathode electrons flow in the n-doped side and are attracted to the anode. The recombination process can further take place reducing the blockade up to its disappearing. In this case the diode is conducting and current can pass through it.

the active medium in the center of them. Photons that travel perpendicularly to the mirrors are reflected and stay in the resonator. These photons then travel through the active medium and when they interact with an excited state atom they stimulate the emission of a photon with the same quantum characteristics as the initial photon. The photons travel many times through the resonator, so that they can stimulate the emission of a large number of additional photons. To let the laser light leave the resonator, one of the mirrors is partially transmissive, so that not all photons get reflected but some of them can leave the resonator and create the light beam of the laser that can be seen outside the laser apparatus.

The diode laser operates on the same principles as an LED itself. The only difference is that the diode is placed between two mirrors that create the resonator. The active medium is the center of the diode, where the recombination of electrons and holes occurs and where the photons are released.

The first step to allow the flow of current in such a laser is to apply a forward

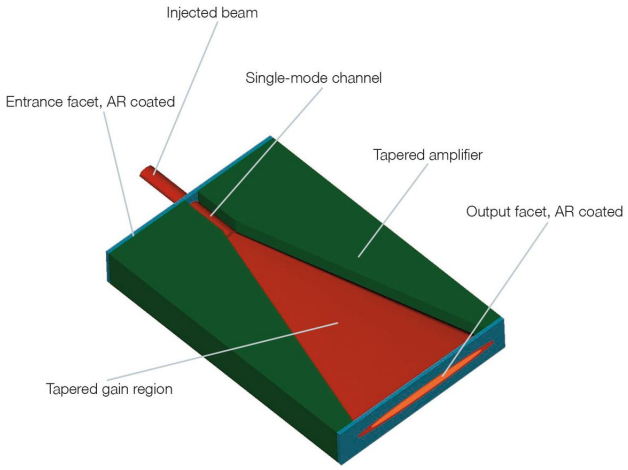

Fig. 4: Schematic of the tapered amplifier. Through the red colored region the waves can propagate; through the upper small red cylinder the light comes from the master laser into the TA. The blue regions are antireflection coated. Through the orange aperture the waves can travel outside the TA. Figure taken from [14].

voltage to the diode. In the active zone the electrons recombine with the holes producing photons. These can stimulate the recombination of more holes and electrons so that more and more photons with the same characteristics are created. This light is reflected by the mirrors of the resonator and further stimulate the generation of electromagnetic radiation. A part of the generated light passes through the partially reflective mirror and creates the light beam of the laser.

The wavelength of the laser light depends on how big the bandgap of the semiconductor and the doping materials used is. There are diode lasers that can produce wavelengths from infrared to ultraviolet, spanning between 375 nm and 2000 nm [15]. Some advantages of this type of lasers include their tunability when used in Littrow configuration or their compact size due to the small size of the diodes. They function reliably over long periods of time and exhibit a high electrical/optical efficiency, up to 65 % [16].
However, there are also disadvantages to these lasers. They cannot achieve such high power values as i.e. CO_2 lasers due to the risk of catastrophic optical damage at high intensities. Applying high intensity currents also poses a risk of degrading the diode. Another issue is their beam profile, which is typically elliptic, resulting in strong beam divergences [17].

If the required power can not be achieved by the diode laser alone, Tapered Amplifiers (TA) are commonly used. The configuration can be seen in Figure 4. A TA is a specialized semiconductor optical amplifier designed to boost the output power of a single-mode diode laser while preserving beam quality. The first part of this optical element is the ridge waveguide. This entrance is very narrow to allow only a single propagation mode per polarization direction, acting as a spatial mode filter. The second part is the tapered section where the light is amplified. Amplification occurs due to the gradual increase in the cross-sectional area where the waves can propagate. Here, the beam can expand horizontally (though not vertically, as the construction does not increase in this direction). To amplify the beam, the tapered section is supplied with pump current via an electrode that covers the tapered region. To achieve amplification, the light from the master laser is guided through the TA. The total gain can reach up to 20 dB, with output power extending up to 4 W [14].

3.3 Spectroscopy

Spectroscopy is a common method used to analyze the electronic properties of different chemical elements, as every atom species has its own properties that define it. One of these properties is the different number of electrons. This is used in spectroscopy to characterize them. This technique consists of a group of physical methods for analysing the radiation of elements or matter according to its properties such as wavelength, energy, etc. In atomic physics it is used to study atoms. This is done by studying electronic transitions through the emission or absorption of light. This technique makes it possible to study a large part of the electromagnetic spectrum, up to 16 orders of magnitude in the frequency range [18]. The main idea of spectroscopy is to measure how photons interact with matter, depending on the energy of the photons, according to the equation $E = h \cdot \nu$ [18].
The spectrum recorded by atomic spectroscopy is discrete, because the energy that an electron can have is also discrete. However, there are some effects that broaden these lines.

- Natural broadening: this occurs due to the finite lifetime of the excited states, which introduces energy uncertainty. This effect results in a Lorentzian emission profile.
- Power broadening: this is an example of homogeneous broadening. This effect gets bigger as the laser power increases. The linewidth of the absorption increases with intensity.
- Pressure broadening: the radiation emitted by a single particle is affected by

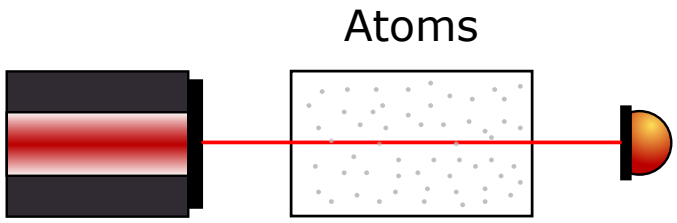

Fig. 5: Typical setup for performing spectroscopic measurements. On the left is the laser that produces the light, which is scanned over a set range of frequencies. This beam of light then travels through the chamber containing the atoms being studied. These atoms absorb light as they undergo atomic transitions. The light can then be detected on the detector, with some frequencies missing that correspond to those that excited the atoms. A legend of the optical elements used for the representation of this setup can be seen in Figure 30.

the presence of nearby particles. Collisions with other particles shorten the emission time, increase the energy uncertainty and cause broadening, which depends on gas density and temperature. The resulting broadening of the linewidth can be described by a Lorentzian profile.

- The Doppler broadening is the one that has the most significant effect. It appears when the atoms of the sample move according to the Maxwell-Boltzmann velocity distribution. Then the atoms can still be excited by a detuned laser when the Doppler effect counteracts the detuning. This causes that the atoms can be excited over a broad range of frequencies. Here the discrete lines merge with each other resulting in a big Gaussian with a width that is on the order of GHz for an atomic beam. This is why there is a method called Doppler-free spectroscopy, or saturation spectroscopy, to improve the absorption spectrum increasing the resolution of it to MHz. This is further explained in subsection 5.1.

Spectroscopy usually requires a light source, a probe and a detector to detect the light. There are broadly speaking two types of spectroscopic techniques:

– Absorption spectroscopy: Here the probe is illuminated with a light source that emits over a range of frequencies. Photons from the laser with frequencies that are resonant to atomic transitions in the sample are then absorbed. A detector measures the loss of light from the laser as a function of frequency. The absorbed frequencies correspond to the electronic transitions of the sample. A scheme of such a setup for absorption spectroscopy is shown in Figure 5.

– Fluorescence spectroscopy: In this method, only the light emitted by the atoms is measured. This requires the atoms to first be transferred to an excited state by absorbing a resonant photon. When they decay to lower energy states, the photons emitted are sent isotropically over all directions. This makes it possible to place the photodiode perpendicularly to the propagation plane of the laser so that only the emitted light from the atoms is detected.

The method used in this thesis is absorption spectroscopy by using lithium atoms. One way to conduct such spectroscopy measurements is to direct laser light into a cell containing the atoms. Those must be in the gas phase, which is achieved by heating them. When the atoms are sublimated, they leave the oven section and form an atomic beam. This atomic beam is perpendicular to the laser beam. If the laser light is in resonance with the atoms - i.e. the frequency of the laser light is the same as the one between two electronic levels of the atom - the atoms can be excited. The frequency of the absorbed photons is then missing from the laser light. This can be detected with a photodiode.
There are also different types of spectroscopy within absorption spectroscopy. Two of them were used in the work of this thesis: Doppler-limited and Doppler-free spectroscopy.

3.4 Doppler-Limited Spectroscopy

Doppler-limited spectroscopy can be performed with a single laser beam, an atom probe and a light detector. The setup used in this thesis to perform Doppler-limited spectroscopy is shown in Figure 5. As the name suggests, this method of spectroscopy is limited by the Doppler effect. This effect occurs when the receiver - the atoms - of a wave perceives a different frequency of the wave than it actually has because it is moving towards (away from) the sender, therefore receiving a higher (lower) frequency. As the atoms in the chamber move, they experience the Doppler effect. Each atom moves at a different velocity according to the Maxwell-Boltzmann distribution, so depending on their direction of movement, they may perceive red-shifted (lower frequency) or blue-shifted (higher frequency) laser light. The shift can be calculated using the Equation 3.2

$$\omega - \omega_a = h \cdot v, \tag{3.2}$$

where ω is the frequency of the laser, ω_a the frequency of the laser with the atoms as the reference system, h is the Planck's constant and v is the velocity of the atoms. If the atoms are regarded as a two-level system, the transition frequency between the ground and excited states can be reached at different laser frequencies

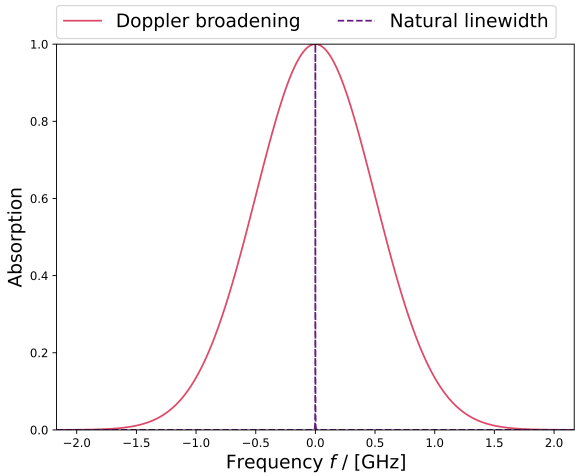

Fig. 6: Absorption line from a Doppler-limited absorption spectroscopy. The Doppler broadening was calculated using Equation 3.3 and setting the temperature T to 400 °C and the mass m to 6.0151228 u for ^{6}Li. The result is a Doppler broadening of $\delta f = 3.38487$ GHz. This value is for a vapour cell where the atoms can move freely.

depending on the speed of the atoms. This broadens the range of frequencies at which the laser is in resonance with the atomic transition. The Doppler broadening can be calculated using the following equation [19]

$$\delta f = \frac{f_0}{c} \cdot \sqrt{\frac{8 \cdot k_\mathrm{B} \cdot T \cdot \ln 2}{m}}, \tag{3.3}$$

where δf is the Doppler shift, c is the speed of light, k_B is the Boltzmann constant, T is the temperature of the atoms and m is their mass.

If the laser light comes from only one direction, as the atoms have a Gaussian velocity distribution in each direction, the absorption spectrum from Doppler-limited spectroscopy has a Gaussian shape, as shown in Figure 6.

In this figure it can be seen that the Doppler broadening is on the order of GHz for temperatures on the order of hundreds of °C. In order to see the hyperfine splitting (which is on the order of MHz), we need to consider other techniques where Doppler broadening does not have such a large effect.

3.5 Saturation Spectroscopy

To overcome the Doppler effect, a different way to do spectroscopy is needed. There are two main requirements for this new spectroscopy method. The first one is two lasers that travel in opposite directions, so that both beams can excite the same group of atoms. And the second requirement is that one of the lasers has to have more power than the other one. The weaker laser beam is the one used for conducting the measurements. A possible setup for conducting this kind of spectroscopy is shown in Figure 7. Here a laser passes once through a chamber where the atoms can be excited if the laser is in resonance with them, this is called the pump beam. The laser then passes through a filter and is reflected by a mirror. On its way back, the beam is attenuated further as it passes through the filter again. This attenuated beam is called the probe beam. This beam then passes through the atomic cloud after being reflected and attenuated. It can now excite the atoms again if the resonance condition is fulfilled. The light is then reflected at the Polarising Beam Splitter (PBS) and reaches the detector. The light beam reflected by the PBS has much less power than the transmitted beam. This can be set with a $\lambda/2$ wave plate, as they are used to set the power of the transmitted and reflected beams splited after a PBS. This can be done because the PBS separates the light depending on its polarization. The $\lambda/2$ plate rotates the polarization direction of the incident beam such that the relative amounts of s- and p-polarized light can be controlled. As a result the power of the reflected and refracted light can be set as desired. There are two main cases of what can happen if the laser is either in resonance with the atomic transition or if it is detuned, i.e. it has a different frequency to that required for the atomic transition. Consider the case where the laser is red detuned, i.e. the frequency is too low to be resonant with the atoms, and the atoms move to the left according to the left diagram in Figure 8.

Due to the redshift of the frequency seen by the atom when it interacts with the strong laser, the transition to the second hyperfine level of the ground state will take place. If the atom interacts with the weak laser, the transition will take the atom to the excited state. If the atom moves to the right, the opposite happens with both lasers. This can be seen in the diagram on the right of Figure 8.

Now consider the case where the laser beam is in resonance with the atoms. In this case, the lasers can only excite the atoms that do not feel the Doppler effect. This means that only the atoms moving in the plane perpendicular to the direction of the laser beams can be excited. The same group of atoms can now be excited by both the pump and the probe laser beam. Since the strong laser beam has more power, a large group of atoms will be in the excited state after the interaction with the strong laser beam. The absorption diagram of the probe laser will have

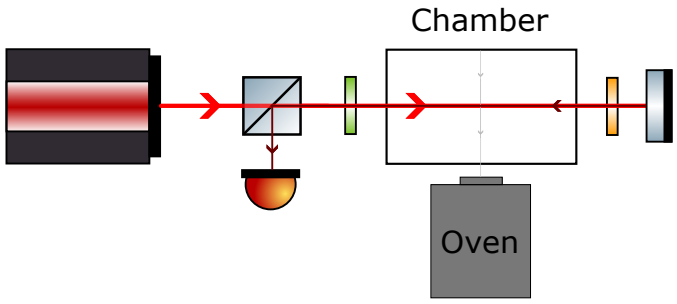

Fig. 7: Schematic setup for performing Doppler-free spectroscopy. On the left, the laser produces the coherent light. This light beam is the pump beam and is transmitted at the PBS to enter the chamber where it intersects with the atomic beam. Here the atoms absorb some of the light. The light is attenuated by the filter, then reflected by the mirror and attenuated again as it passes through the filter. This is the probe beam that can excite some atoms while it passes through the chamber. At the PBS, the probe beam is reflected so that it can reach the detector. A legend of the optical elements used for the representation of this setup can be seen in Figure 30.

a dip, called the Lamb dip, at the resonant frequency because most of the atoms are already in the excited state due to the pump laser. The weak laser light will pass through the atomic ensemble without losing many photons because there will be fewer atoms to excite.
For atoms with a three-level scheme, other dips and peaks may appear in the absorption diagram. For the case where the atom has two hyperfine-split excited states and a ground state, like in Figure 9, a cross-over dip will appear in the absorption spectrum of the probe beam. This follows the same reasoning as for the Lamb dips, the only difference being that this happens with atoms that are not at rest. As the laser beam does not resonate with the atomic transition, the atoms that can be excited are moving and feel the Doppler effect. This means that there are two velocity-distributed groups of atoms, one moving to the left and one moving to the right, which are in resonance with the pump and probe beams. Since both lasers are in resonance with both groups of atoms, they are more likely to undergo the transition when they interact with the pump beam. When the atoms then interact with the probe beam, there will be fewer ground state atoms left, so the absorption of the probe beam will be much lower than it would be if the pump laser was not shining on the atoms. A cross-over dip can then be seen in the absorption spectrum. In atoms with more than three levels the effect of the cross-over can also be seen. It appears between all the transitions that have common ground or excited states. An atomic species where this effect also appears is rubidium [21].

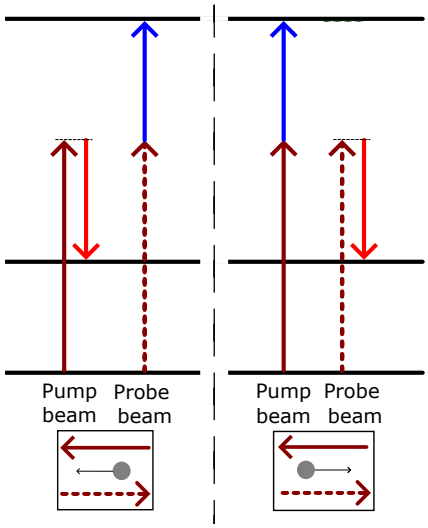

Fig. 8: Energy diagram of a three-level atom. There are two shared ground states and one excited state. On the left side of the diagram the atoms are moving to the left. They are blue detuned with respect to the probe beam. This causes them to undergo the transition to the excited state when they interact with the probe laser. But they are also detuned red with respect to the pump beam, so they can make the transition to the second ground state when they interact with the pump beam. This only happens if the atoms have the right velocity, so that the blue or red Doppler shift counteracts the detuning of the laser. The same principle applies to atoms moving to the right with the effect of each beam reversed.

3.6 Optical Density

To quantify how much of the light is absorbed by the atoms, the optical density can be calculated. This is defined as the absorbed light over a distance Δz [22]:

$$OD = \alpha \Delta z \tag{3.4}$$

This is defined employing the Lambert law [22]:

$$I(z) = I_0 \exp(-\alpha z), \tag{3.5}$$

where $I(z)$ is the distance-dependent intensity of the beam, I_0 is the intensity which the beam had initially and α is the intensity-independent absorption coefficient, when the condition $I << I_{\text{sat}}$ is fulfilled. I_{sat} is the laser intensity needed to saturate the atoms, meaning that most of them are in the excited level and can not absorb more photons. The population density proportional coefficient α can

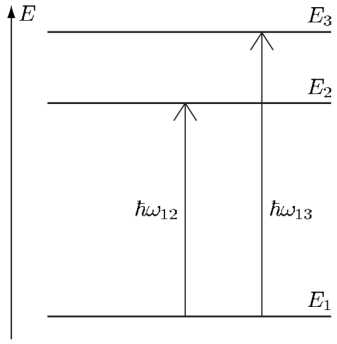

Fig. 9: Energy diagram of a three-level atom with two excited states and one ground state. When conducting saturation spectroscopy on atoms with such a level scheme, a cross-over dip will appear. Figure taken from [20].

be calculated with following equation [23]:

$$\alpha \overset{I << I_{\text{sat}}}{=} n \cdot \sigma_0, \tag{3.6}$$

where n is the density of the atomic cloud and σ_0 is the scattering cross-section, which for a two level atom can be calculated with

$$\sigma_0 = 3\lambda^2/2\pi, \tag{3.7}$$

where λ is the wavelength of the incident light. Since α is related to population density, optical density correlates with the density of the medium and can be used as a measure of it.

3.7 Pound-Drever-Hall Lock

For efficient cooling of specific atomic species their electronic transitions have to be addressed precisely with lasers. Their light must be at the correct wavelength, and therefore frequency, to obtain optimal results. The primary laser for this thesis, which drives the D1 transition of lithium, will be used for an optical molasses. This laser needs to have a precise wavelength to effectively cool the atoms. If the laser is slightly detuned in respect to the atomic transition frequency, this will result in less cooling power, which can reduce the damping force exerted on the atoms. Consequently, higher equilibrium temperatures are obtained. Also temperature drifts and air pressure changes can produces drifts in the laser when no active compensation is used. A robust stabilization technique is therefore essential to maintain the precise frequency required for an effective optical molasses and to ensure consistent cooling and confinement of the lithium atoms.

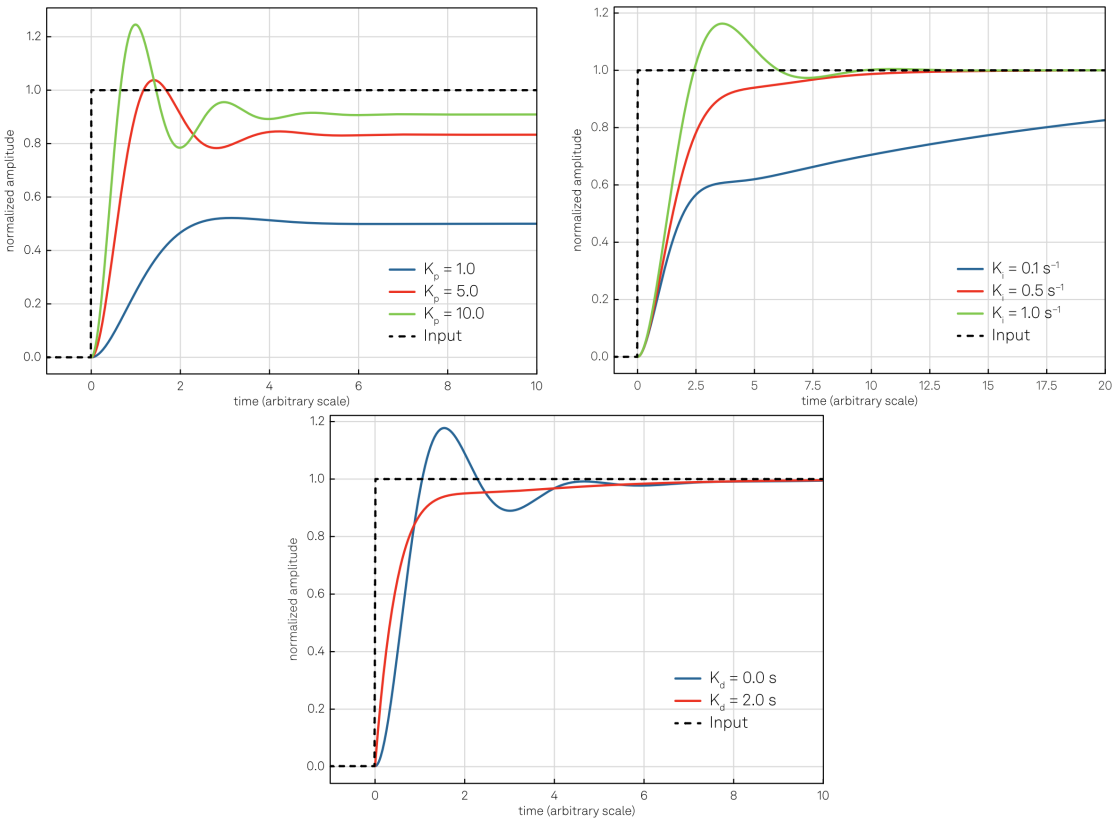

Fig. 10: Curve after applying the proportional module (left plot), the integral module (right plot) and the derivative module (lower plot) with different values of K_P, K_I and K_D respectively. It can be seen that the desired value is reached faster after implementing the three different controllers. Figures taken from [24].

One of the techniques used to stabilize the frequency of a laser is the Pound-Drever-Hall (PDH) locking method. This is an excellent technique for improving laser frequency stability. The main idea of this method is to generate an error signal, as the difference between the setpoint and the actual value, which provides feedback when the frequency needs to be increased or decreased. This is then used as input to a Proportional Integral Derivative (PID) controller, which adjusts laser parameters such as the laser piezo element and current to keep the laser at the correct wavelength.

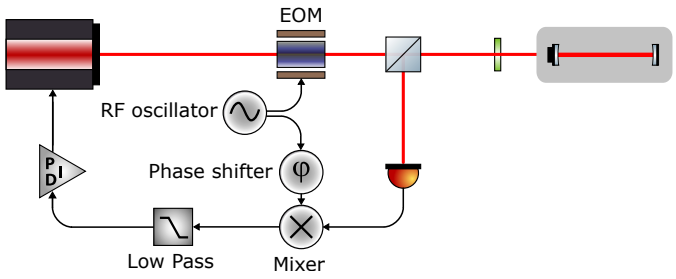

Fig. 11: Schematic diagram of the elements required to perform a PDH lock. A legend of the optical elements used for the representation of this setup can be seen in Figure 30.

3.7.1 Processing the Error Signal with the PID Controller

The PID controller is a summation of three different elements, the proportional controller, the integral controller and the derivative controller. The proportional controller multiplies the error signal by the factor K_P. This means that the error of the output will still be large because this process requires an error to generate the proportional response. This can be solved by implementing the integral controller. The integral term is calculated over the past values of the difference between the setpoint and the actual value, so if there is still a difference between the two values after the proportional controller is applied, the integral term removes this residual error by incorporating a control action based on the accumulated error over time. Some controllers only have these two modules, but a third can also be implemented to give a better output signal. This is the derivative controller, which calculates how fast the signal is changing so that it does not change too fast. Normally, the actual value reaches the setpoint by changing the values of the actual value around the value of the setpoint. The derivative controller can be used to flatten this curve so that the setpoint is reached more quickly.
In Figure 10 the change in the actual value can be seen after adding the various controllers to modulate the output signal.
After the signal has been processed in the PID controller, the parameters that need to be changed are fed back to the laser. With this information and well-chosen parameters, the wavelength of the laser remains constant at a given value.

3.7.2 Creation of the Error Signal with the PDH Technique

A complex set of optical and electrical devices is required to generate the error signal. A diagram of the equipment required can be seen in Figure 11.
The laser light must be processed in order to produce the desired error signal. The

electric field of the incident laser light can be described as follows [25]:

$$E_{\text{inc}} = E_0 \exp(i\omega t), \tag{3.8}$$

where E_0 is the amplitude of the electric field, i the imaginary number and t represents the time.
The first step in PDH locking is to phase-modulate the light beam to add sidebands at the frequencies $\omega \pm \Omega$. This is done using an electro-optical modulator (EOM). The light with the sidebands is then described as [25]:

$$E_{\text{inc}} = E_0 \exp[i(\omega t + \beta \sin \Omega t)], \tag{3.9}$$

where β is the modulation depth. This equation can be extended using the Bessel functions to [25]:

$$\begin{aligned} E_{inc} &\approx [J_0(\beta) + 2iJ_1(\beta) \sin \Omega t] \exp(i\omega t) \\ &= E_0[J_0(\beta) \exp(i\omega t) + J_1(\beta) \exp[i(\omega + \Omega)t] - J_1(\beta) \exp[i(\omega - \Omega)t], \end{aligned} \tag{3.10}$$

where Ω is the phase modulation frequency and J_n are the Bessel functions of nth kind. The power of the incident beam can then be calculated as $P_0 \equiv |E_0|^2$.
This modulated beam travels from the EOM to an Ultra Low Expansion (ULE) cavity [26]. In the ULE, the frequency of the electromagnetic wave of light has to be an integer multiple of the Free Spectral Range of the cavity ($\Delta\nu_{\text{FSR}} \equiv c/2L$) in order to be reflected constructively. All other wavelengths interfere destructively. Therefore, this element acts as a spectral filter, clearing out all the wavelengths that do not fulfill this characteristic. To characterize the reflection of the beam in the cavity, the reflection coefficient $F(\omega)$ can be calculated. It gives the ratio between the incident beam E_{inc} and the reflected beam E_{refl} [25]:

$$F(\omega) = \frac{E_{\text{ref}}}{E_{\text{inc}}} = \frac{r\left(\exp\left(\frac{i\omega}{\Delta\nu_{\text{FSR}}}\right) - 1\right)}{1 - r^2 \exp\left(\frac{i\omega}{\Delta\nu_{\text{FSR}}}\right)}, \tag{3.11}$$

where r is the amplitude coefficient of each mirror. The formula works for a symmetrical cavity with no losses.
The power of the reflected beam is measured by the photodiode and can be calculated as [25]:

$$\begin{aligned} P_{\text{ref}} &= |E_{\text{ref}}|^2 \\ P_{\text{ref}} &= P_c|F(\omega)|^2 + P_s\left\{|F(\omega+\Omega)|^2 + |F(\omega-\Omega)|^2\right\} \\ &\quad + 2\sqrt{P_cP_s}\left\{\text{Re}\left[F(\omega)F^*(\omega+\Omega) - F^*(\omega)F(\omega-\Omega)\right]\cos\Omega t\right. \\ &\quad \left.+\text{Im}\left[F(\omega)F^*(\omega+\Omega) - F^*(\omega)F(\omega-\Omega)\right]\sin\Omega t\right\} + (2\Omega \text{ terms}), \end{aligned} \tag{3.12}$$

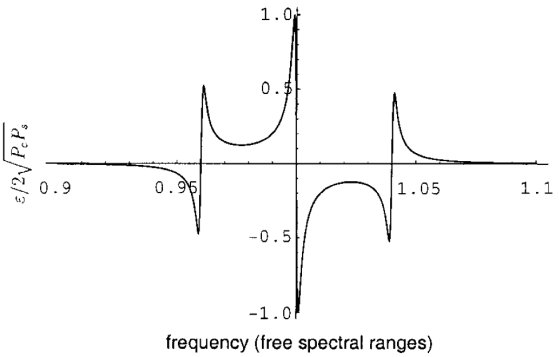

Fig. 12: Error signal in high modulation frequencies. Figure taken from [25]. The x-axis is normalized.

where Re is the real part and Im is the imaginary part of the equation written in brackets. The reflected beam is a coherent sum of two beams: the promptly reflected beam, which is reflected by the mirror at the entrance of the cavity, and the leakage beam, which is a small fraction of the beam reflected in the cavity that leaks back through the partially transmissive mirror at the entrance. These two beams have the same frequency, are in resonance and have the same intensities, but their relative phase depends on the frequency of the beam. The signal of this beam then gets multiplied at the mixer with the same sinus wave used to modulate the EOM. This ensures that almost all terms of Equation 3.12 oscillate. Only the sinus term gives a constant term when multiplied with another sinus, which is the only one that gets through the low pass. As only the first order terms in $F(\omega)$ need to be considered, the emerging signal can be described with following equation [25]:

$$\epsilon = -2\sqrt{P_c P_s}\,\mathrm{Im}\left\{F(\omega)F^*(\omega+\Omega) - F^*(\omega)F(\omega-\Omega)\right\}. \tag{3.13}$$

The plot of this signal can be seen in Figure 12. It has the desired zero crossing required for laser locking and can therefore be used as an error signal for the PID. This method provides a good error signal for laser stabilization, independent of laser power fluctuations and cavity fluctuations. The only disadvantage is the need for a ULE cavity or other cavity stabilization measures, as an active modulation of the cavity length [27].

4 Setup of the Laser System

Diode lasers are essential to many experiments because of their efficiency and compact size. In addition their tunability allows for scanning over multiple GHz and general operation over up to tens of nanometers. Because of these advantages the laser used to drive the D1 transition of lithium is a diode laser. In order to effectively use the light of a diode laser in an experiment, the laser system and optics have to be set up first. To do this, it is necessary to study the optimal parameters for achieving the desired output, which is the subject of this chapter.

4.1 Characterization of the Laser

As our laser source we use a comercial laser system[1] from *Toptica*. The system is comprised of a seed laser running at 671 nm and a Tampered Amplifier (TA) to increase the otherwise low output power of the diode laser. Both the seed laser and the TA are controlled with a *Toptica* analog controller. While the TA is kept at 20 °C at all times, the seed laser temperature can be adjusted to achieve the desired wavelengths. It should be noted, however, that temperatures below 15 °C can lead to water condensation on the diode and the higher the temperature, the shorter the life of the diode. The seed laser has a threshold current of 95 mA, still the current should be kept above 120 mA as this is the current where the TA receives the minimal required input power. The maximal current of the seed laser is 150 mA. The TA can be operated with a current of up to 905 mA.

Although the overall output power depends on both the seed laser and TA current, only the TA current is varied as changes to the seed laser current also change their wavelenght. The efficiency of the TA additionally depends on how well the seed laser beam is aligned through the TA chip. This alignment can be changed by four mirror screws in the laser housing, which were optimized after taking the laser into operation. A laser power vs. TA current curve was measured to see how well the laser performs compared to the data sheet given by *Toptica*. This measurements curve is plotted in Figure 13. A maximal power of 445 mW could be measured. The data sheet gives a maximal achievable power of 525 mW. One of the main reasons for this difference is that the *Toptica* laser was optimized for a wavelenght of 671.1 nm, while we run the laser at a wavelength of 670.992 nm, as well as the age of the laser. The wavelength of the laser is dependent on its operating current, temperature, and grating angle. The grating has the strongest

[1] Toptica TA pro-2V0-13306

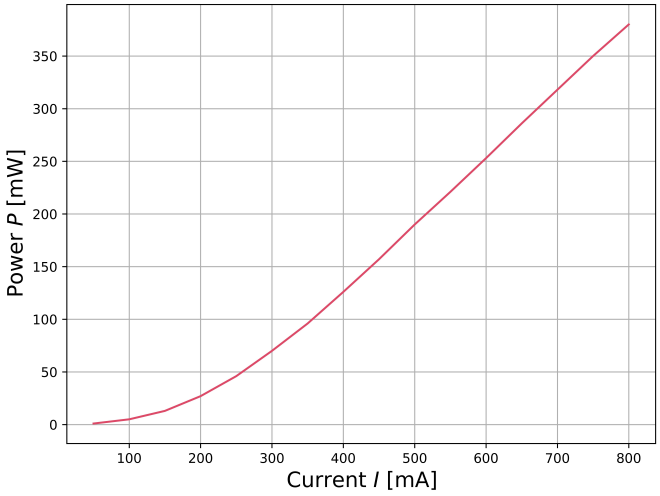

Fig. 13: Laser power versus TA current of the laser system. The curve takes the expected values and the power increases as the applied current increases.

effect on the wavelength and can be used for coarse tuning. For intermediate tuning ranges, the temperature of the seed laser can be used. Fine tuning can be achieved either by the driving current of the laser or by applying a voltage to the gratings in built piezo crystal, which induces very small shifts in the grating angle and therefore frequency of the laser. This is done in a scanning module in the laser's analog controller, which can be used to either apply a constant offset or scan the laser over a range of frequencies.
The temperature dependence of the wavelength of the laser is plotted in Figure 14. The plot shows the typical mode jumps of a diode laser, which occur due to a different expanding rate of the gain curve and the cavity modes. The gain curve describes how the gain of light changes at different wavelengths. The cavity modes are the specific frequencies at which the laser can operate. As the temperature rises, these two characteristics do not increase at the same rate, so there are some wavelengths that the laser cannot reach, so it jumps between the ones it can. The maximal change in the wavelength achieved by changes to the temperature is 0.05 nm.

4.2 Characterization of the Beam Profile

As all laser light will eventually be coupled into single mode fibers, it is advantageous for the beam shape to be Gaussian. Only the Gaussian mode TEM_{00} can be transmitted by single mode fibers which means that any non Gaussian components of the beam will be lost leading to a loss in power. Diode lasers typically have an

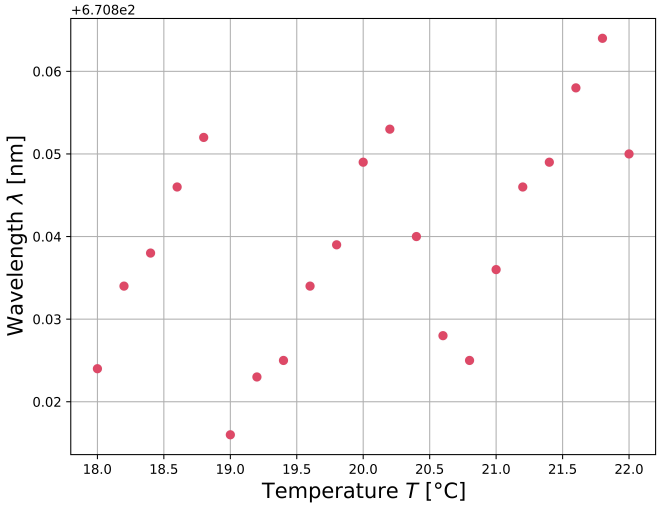

Fig. 14: Measured laser wavelength as a function of the seed laser temperature. The mode jumps at different laser temperatures can be seen.

elliptical transversal beam profile and TAs commonly lead to a decrease in beam quality. To ensure a more uniform beam profile optical elements can be used in a process called "beam shaping".

First the beam profile of the seed laser was observed by using a beam camera[2], which can be seen in the upper left part of Figure 15. The profile shows the expected ellipticity of a diode laser. The beam is then sent into the TA. The emerging profile after the TA can be seen in the upper right part of Figure 15. Here, the profile shows a strong interference pattern. Comparing the recorded beam profile to the one given in the data sheet by *Toptica* the interference pattern can also be seen. However, in the recorded data the maxima and minima are stronger pronounced and more plentiful. The beam profile after the TA given in the datasheet is in the lower part of Figure 15.

Suspecting that the interference pattern of the beam might come from a higher order spatial mode in the laser resonator dependence of the beam profile was checked in relation to the temperature and operating current of both the seed laser and TA. However, regardless of which parameters were chosen the beam profile remained the same. As no improvement could be achieved by changing these parameters, instead the emerging beam profile has to be changed by beam shaping.

First attempts to couple the the light into a single mode fiber showed that only

[2]DAT-WinCamD-LCM from Dataray

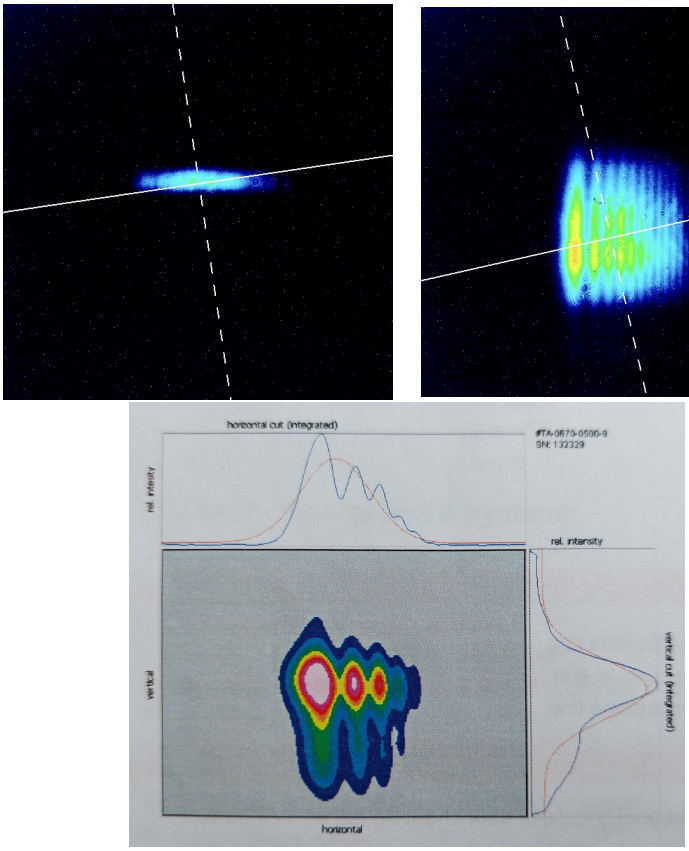

Fig. 15: The left picture shows the beam profile of the laser beam at a distance of 75 cm after the laser opening. The right picture shows the beam profile of the seed laser, before passing through the TA. The lower picture shows the beam profile of the data sheet from *Toptica*.

one of the maxima in the interference pattern can be coupled at a time. This corresponds to a coupling efficiency of less than 2 %. Therefore, two anamorphic prism pairs are used to reshape the strongest maximum to a more Gaussian shape. An anamorphic prism pair can be used to reshape a laser beam, either widening it or, as in this case, narrowing it in the desired direction by changing the position of the input and output beams. After including only one prism pair the power of the beam was too spread out, as it can be seen in the left picture of Figure 16. This is why another prism pair was included to shape the power into a more Gaussian-like spot. This can be seen in the right picture of Figure 16. The strongest maxima looks more Gaussian and focused than in the beginning. With this double prism pair configuration a coupling efficiency of 40 % could be achieved.

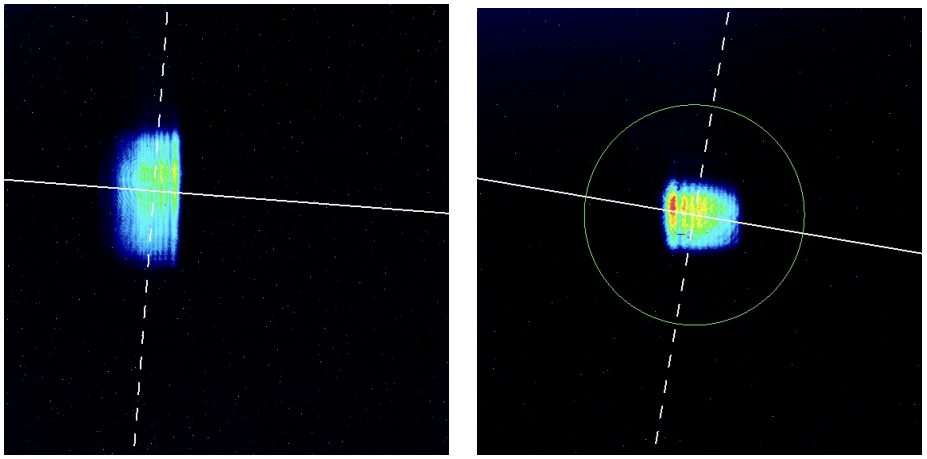

Fig. 16: The left image shows the beam profile after passing through a pair of anamorphic prisms. It can be seen that the beam has been reduced in size in the horizontal direction. The right image shows the beam profile after passing through a second pair of anamorphic pair of prisms, where the beam size has been reduced to approximately 25 % of the total original size. This allows the compression of the maxima and minima to produce a beam with a more Gaussian shape.

Finally, before being coupled into the fiber the laser passes through a $\lambda/2$ wave plate. This is done to achieve polarization maintaining coupling, which requires the light polarization to be aligned with respect to the optical axis of the fiber. The setup for beam shaping and coupling is shown in Figure 17.

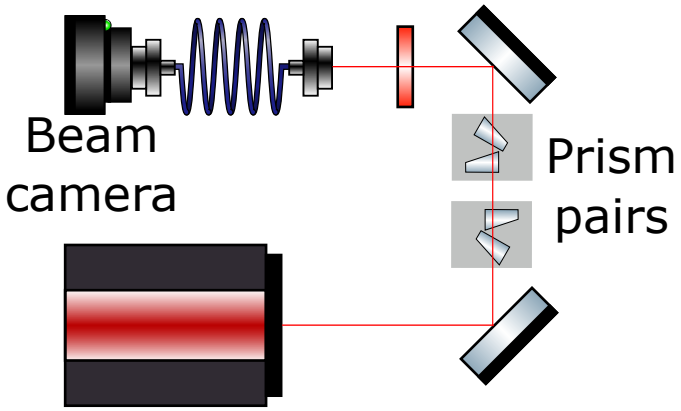

Fig. 17: Schematic drawing of the setup for the measurement of the beam profile. For the first measurements, where only the characteristics of the laser such as temperature or current changes (see Figure 13 and Figure 14), the camera was placed direct at the opening of the laser. For the two measurements of the beam after one and two prism pairs (see Figure 16) the camera was placed after the first and second prism pair, respectively. A legend of the optical elements used for the representation of this setup can be seen in Figure 30.

Two different lasers are used in this work for driving the D1 and the D2 transition of lithium. Although the second transition of lithium is only 10.5 GHz away from the D1 transition, as shown in Figure 2, another laser is needed to excite the atoms to the second excited state $2^2P_{3/2}$. This laser works in a different way to the D1 laser. The output light of the seed laser has a wavelength of 1342 nm. This light goes into a polarisation-maintaining fiber, which is connected to a fiber amplifier where the light is amplified. The frequency of the light is then doubled by a Second Harmonic Generation (SHG) crystal [28], which converts the near-infrared seed light into a 671 nm light. This laser system was already set up, and will be used for the D2 spectroscopy in the following chapter.

5 Spectroscopy of Lithium

This section presents the results of spectroscopic measurements on lithium using the lasers that drive the D1 and D2 transitions. In the following, both lasers are named after the transitions they drive. These are part of the measurements required to keep the laser at a constant wavelength, i.e. to perform a laser lock. The parameters set in section 4, such as power and temperature, allowed the laser to be roughly at the desired wavelength, but it can be seen that small perturbations or natural laser drift change the frequency of the laser over large ranges, as in Figure 14. To stabilize the frequency of the laser, it must be locked. The theory behind laser locking has been explained in subsection 3.7, and how it is done in detail for the D1 and D2 lasers is explained in section 6. However, the locking frequency of the laser has to be known. For this the ULE peaks are taken as a reference in a relative frequency scale. Then the exact frequencies of the transitions relative to the ULE are investigated via spectroscopy measurements. After their frequency is measured, the absolute frequency at our wavemeter is known and can be used for later locking. This work focuses on absorption spectroscopy.

Within absorption spectroscopy there are two main methods that can be performed, Doppler-limited and Doppler-free or saturation spectroscopy. It depends on the required resolution which of them is used. The theory behind this two techniques is explained in section 5. In this work, both of them have been carried out. How the measurements were performed and the recorded spectra are the subject of the next sections.

5.1 Doppler-Limited Spectroscopy

This chapter presents the results obtained by performing Doppler-limited spectroscopy on lithium. The main idea is to shine a laser beam into the atomic sample to excite the atoms. The frequencies of the light absorbed by the atoms as they transition to the excited state are then missing in the laser light and can be detected by a photodiode. This method is limited by the Doppler effect because the atoms move with different velocities given by the Maxwell-Boltzmann distribution due to their finite temperature. This means that at laser frequencies other than the resonant frequency, the atoms can still be excited if the Doppler effect can counteract the laser detuning. Consequently, the resonant frequency detected by the photodiode is broadened. The broadening effect is usually on the order of GHz, which is why this kind of spectroscopy only seems to show a single main peak in the absorption. This is because the hyperfine splitting of the lithium transitions

is way smaller than the Doppler broadening, which leads them to overlap with each other to one single peak.

5.1.1 Setup

Different setups were built for the spectroscopy measurements with each laser (D1 and D2). The main components for performing this experiment are the laser, the oven, and the ULE. The laser is either the D1 or D2, since both lasers were used for spectroscopy. The oven is a dual-species oven that can produce both rubidium and lithium atomic beams. In this thesis it is used for lithium only. The design and construction of this oven has been described in [9]. The ULE is a special type of cavity designed to minimize any expansion or contraction of the resonator mirrors due to external influences such as temperature or pressure changes. To achieve this it is kept under vacuum. In the ULE, when the beam is perfectly aligned, only wavelengths that are an integral multiple of twice the cavity length are able to propagate. These are seen as peaks separated by the so-called free spectral range (FSR) and represent the frequencies that constructively interfere within the cavity [25].

$$\Delta\nu_{\mathrm{FSR}} \equiv c/2L, \tag{5.1}$$

where ν_{FSR} is the Free Spectral Range (FSR) [29] of the cavity, c is the speed of light, and L is the length of the cavity. This is the reason why the signal of the transmitted beam shows the main peaks separated by the FSR of the cavity. The FSR of the cavity can be determined by Equation 5.1 and is 1.498 GHz for the cavity used in this experiment. This can be used as a reference signal to determine relative frequencies very precisely, e.g. for laser locking.

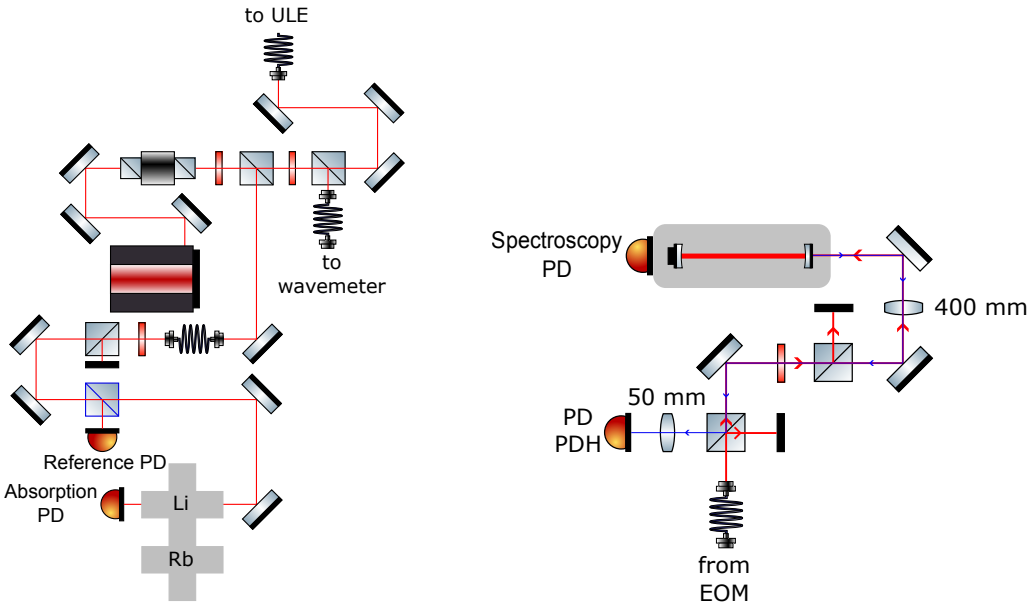

Fig. 18: The schematic on the left shows the setup for performing Doppler-limited spectroscopy with the D2 laser. The laser light exits the laser, passes through an optical isolator, and is split into one beam that goes to the ULE and another beam that goes to the oven. There are several $\lambda/2$ plates to adjust the power of the splitted beams in the PBS. To the right is the ULE setup. Here, the light shown as the beam shown in red comes from the fiber in the lower center of the scheme. It travels to the cavity where it can propagate if the resonance condition is met. The transmitted beam gets detected by the spectroscopy photodiode. A legend of the optical elements used for the representation of this setup can be seen in Figure 30.

The left picture in Figure 18 shows the setup with the D2 laser and the Li-Rb oven. The beam exits the laser housing and is separated at the first PBS to travel to the lithium oven and the ULE. This second beam is sent through a fiber to the ULE and then takes the path shown in the right image. Here, the incoming beam goes to the cavity (shown as the red beam) and the transmitted light is recorded with the spectroscopy photodiode. The beam traveling to the oven is sent down a fiber and split for polarisation cleaning with a PBS. One beam gets further split at a 50:50 BS. One of the split beams travels to the lithium oven where it interacts with the atoms and is then recorded by a photodiode. The other beam is recorded before it interacts with the lithium atoms and is used as a reference to determine the difference between the signal from the light that interacts with the atoms and the light that does not. The $\lambda/2$ waveplates are used to set the power of the transmitted and reflected beams when they get split at a PBS. In this thesis, the

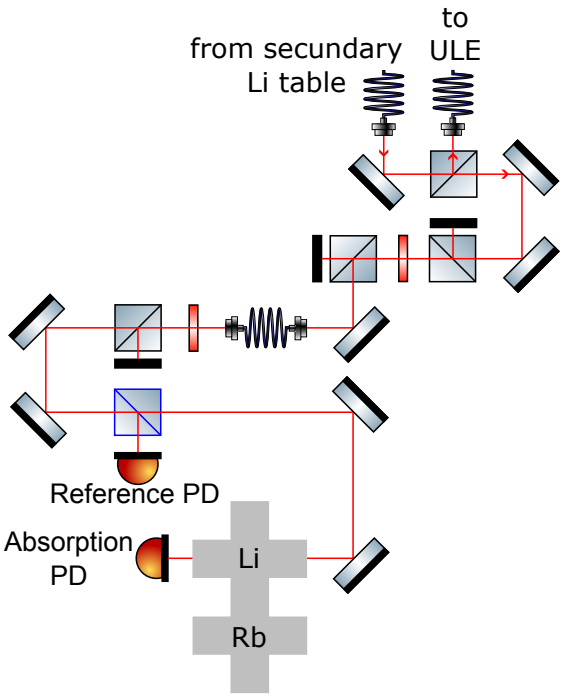

Fig. 19: Representation of the setup of the main lithium table for performing Doppler-limited spectroscopy with the D1 laser. The light comes from the upper left fiber and is split at the first PBS into a beam that goes to the ULE setup and another beam that goes to the oven for performing the spectroscopy. The setup of the D2 laser is used, so there are some elements that are not used for that laser. The $\lambda/2$ wave plates are used to adjust how much power is transmitted or reflected in each PBS. A legend of the optical elements used for the representation of this setup can be seen in Figure 30.

setup on the left in Figure 18 is called the main lithium table and the setup on the right is called the ULE setup.

The setup for performing Doppler-limited spectroscopy with the D1 laser differs from the setup for the D2 laser shown in the left image. The setup for the D1 laser is shown in Figure 19. The ULE setup remains the same for both lasers, only the fiber has to be changed to switch the laser light. For the D1 laser, the beam profile corrections described in subsection 4.1 were implemented in the setup. The laser light is then splitted in one beam that goes to the wavemeter, used to have a reference of what wavelength the wavemeter is recording when the laser light is in resonance with the atoms, and another beam that goes to the main lithium setup.

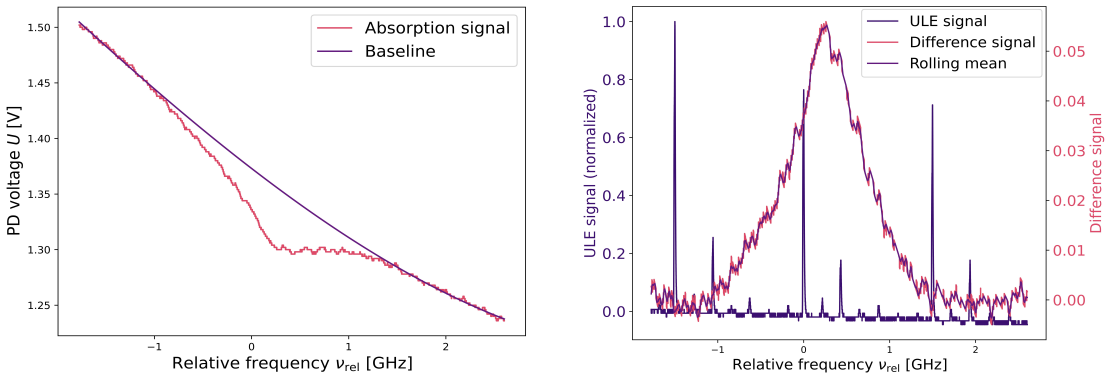

Fig. 20: On the left the absorption line of Doppler-limited spectroscopy performed with the D2 laser is shown. The absorption peak can be seen by comparing the curve of the absorption signal and the fitted baseline. On the right plot the difference signal from the baseline and the absorption signal is represented. In the figure the rolling mean from the difference signal has been plotted to see the curve more clearly. The ULE signal, which has been used to establish the relative frequency scale, has also been plotted

To perform the spectroscopic measurements, the lithium oven must first be heated. The temperature has to be high enough to have a high enough density of lithium atoms to have a good signal. For these measurements it was set to 450 C°. Then the laser is turned on. The electronic transitions have very specific wavelengths, but since the experiment is Doppler-limited, these discrete values are grouped into a range of frequencies where the atoms can be excited by the laser light. To find which ones are resonant, the laser is scanned over a wide range of frequencies around a given value, which can be set by adjusting the offset. Both the offset and scan amplitude can be set with a *Toptica* scanmodule[3].

5.1.2 Results

After conducting the experiment, the results seen on the oscilloscope can be processed and evaluated.

D2 laser

The absorption curve of the Doppler-limited spectroscopy using the D2 laser can be seen in Figure 20 and the one from the D1 laser in Figure 21. In Figure 20

[3]Toptica SC110

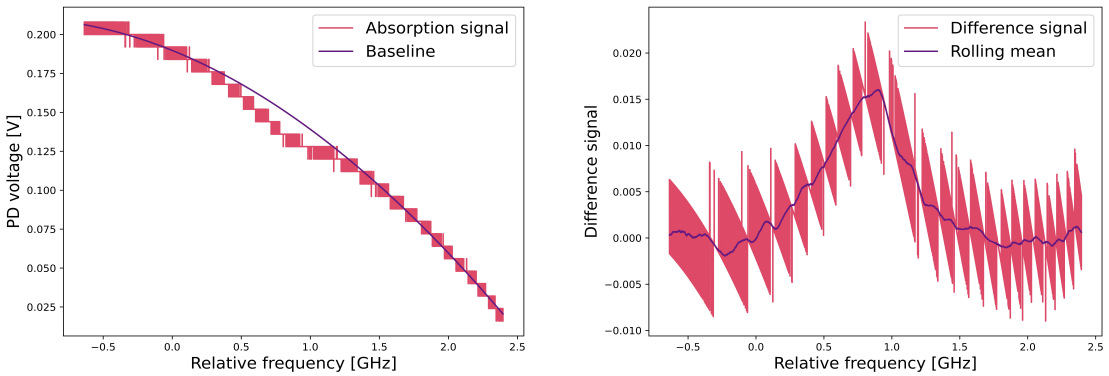

Fig. 21: The left plot represents the photodiode signal for the Doppler-limited spectroscopy using the D1 laser. Both plotted curves, the absorption signal and the baseline are subtracted in order to represent the difference signal that can be seen on the right plot. The difference signal represents the absorbed light by the atoms. In the figure the rolling mean from the difference signal has been plotted to see the curve more clearly.

it can be clearly seen the Doppler broadened absorption dip of the red curve using the D2 laser. The purple line describes the laser light that does not interact with the atoms. The scanning range of the laser during these measurements was from 446.7971 to 446.8023 THz, or from 670.981 nm to 670.973 nm, at our wavemeter. The right plot shows the difference signal, which describes how much light the atoms absorb from the laser light. The Doppler broadening is about 2 GHz. The difference signal on both Figure 20 and Figure 21 has not the typical Gaussian shape of the Doppler-limited spectroscopy because the measurement was conducted with a non-isotropic atomic beam [30]. This is also the reason why not so high densities can be reached and thus why the signal is weak, compared to a vapor cell [31]. Additionally, the ULE signal has been plotted to represent the chosen relative frequency scale. This applies to all spectroscopy measurements. The higher order peaks from the ULE can also be seen.

D1 laser

For the Doppler-limited spectroscopy of lithium using the D1 laser, the absorption curve is plotted in Figure 21. On the left plot from Figure 21 the small dip between 0.3 and 1 GHz can be seen. This corresponds to the absorption of the laser light by the atoms. In the right diagram the difference signal between the absorption and the baseline of the left plot are represented.

5.2 Saturation Spectroscopy

In order to get a better resolution and be able to resolve the hyperfine substructure to get a better knowledge of the frequencies at which the atoms are excited, Doppler-free spectroscopy has to be performed. Here, two counter propagating beams with different intensities but same frequencies are used. The atoms are first excited by a strong beam, called pump beam. Then they interact with a weaker beam, called probe beam, and since a large fraction of the atoms are already in the excited state, the interaction with the probe beam cannot excite them further. This creates a small dip, called Lamb dip, in the absorption curve of the probe beam, which is on the order of MHz, meaning that this spectroscopic method can resolve the hyperfine structure of the ground state of lithium as it has a spacing of 228.2 MHz (see Figure 2). This only happens when both beams have the same frequency, because then they are resonant with the same group of atoms. This group of atoms includes those that move perpendicular to the laser propagation and therefore do not show broadening due to the Doppler effect. If the laser light is detuned red, the atoms will resonate with the beam they are moving toward. If the light is blue detuned, the opposite happens.

Additional dips and peaks can occur in a three-level system. The energy level scheme of lithium can be simplified to look like the three-level atom with two ground states and one excited state as shown in Figure 22. In such atoms a cross-over peak appears due to a compensation of optical pumping of the probe beam. For clarity, in the following the two ground states of the system will be called $|g_1\rangle$ and $|g_2\rangle$, and the excited state $|e\rangle$, respectively. The absorption profile of the probe beam is generally slightly decreased due to optical pumping from one ground state to the other, even without the effects of the pump beam taken into consideration. If the probe beam is resonant to the transition from the $|g_1\rangle$ to the $|e\rangle$ states, for example, population will accumulate in the $|g_2\rangle$ state as $|e\rangle$ can decay into both ground states. A cross-over peak occurs when both the probe and beam laser have a frequency that lies exactly between the cies from the $|g_1\rangle$ to $|e\rangle$ and from $|g_2\rangle$ to $|e\rangle$ transitions. In this case, the probe beam can excite atoms from both $|g_1\rangle$ and $|g_2\rangle$, however, only a specific velocity class +v in $|g_1\rangle$ and -v in $|g_2\rangle$ can be excited because of the Doppler shifts involved. As the pump beam goes in the inverse direction of the probe, the Doppler shifts are inverted. The pump beam only excites atoms of velocity class -v in $|g_1\rangle$ and +v in $|g_2\rangle$. This means that although both probe and pump beam drive both transitions, they speak to completely different velocity classes in those states. Therefore the pump beam does not lead to the typical decrease in probe absorption known from the lamb dips in Doppler-free absorption spectroscopy. In fact, the effect of the pump beam

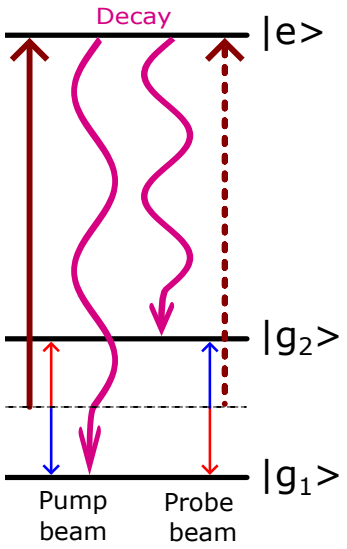

Fig. 22: This plot shows a three-level energy system diagram in which an absorption or cross-over peak appears in saturation spectroscopy. This peak appears due to the increased absorption of the probe beam caused by the population increase in the energy level addressed by the probe beam. The population increase is due to the decay of the atoms excited by the pump beam. The decay can be to the upper or lower ground state, so both possibilities are described by the photon arrows.

even enhances probe absorption: it brings atoms lost to the aforementioned optical pumping of the probe beam back into the excited state and therefore transition cycle, functioning effectively as a repumper to the probe transitions. This can be seen as an absorption peak in the signal between two lamb dips.

5.2.1 Setup

To study saturation spectroscopy, the experimental setup has to be changed slightly. In Doppler-limited spectroscopy, the light interacts with the atoms and is immediately detected by a photodiode. For Doppler-free spectroscopy, however, two beams of different power need to overlap. This can be achieved by replacing the photodiode at one end of the oven with a mirror. The probe beam is created by placing a filter in the path of the reflected beam that attenuates the light as it passes toward the mirror and as it is reflected. The setup is shown in Figure 23.

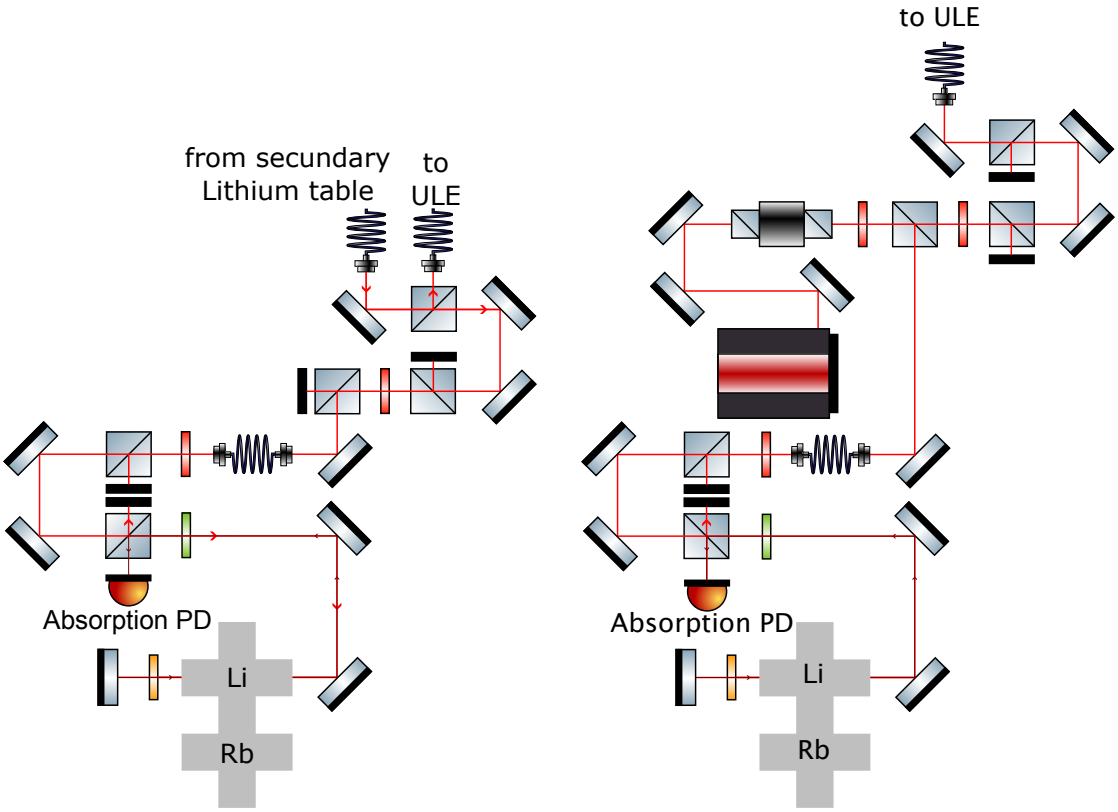

Fig. 23: The left diagram shows the setup for performing saturation spectroscopy with the D1 laser. The light comes from the secondary lithium table where the D1 laser is placed. It is then split into a beam that goes to the ULE setup shown in Figure 18 and one that goes to the oven where the spectroscopy is performed, this is the pump beam represented in light red. An ND1 filter and a mirror are placed on the left side of the oven. The filter attenuates the reflected light to create the probe beam, represented in dark red. The right diagram shows the setup for the D2 laser. Again, the light is split into two beams for the ULE setup and the oven. The probe beam, represented in dark red, is detected at the photodiode after the light is reflected at the last PBS. A legend of the optical elements used for the representation of this setup can be seen in Figure 30.

The procedure for performing the measurement is the same as for Doppler-limited spectroscopy. Here, the laser is also scanned over a range of frequencies, set with the amplitude button in the module[4], around a given value, set with the offset on the same controller.

[4]SC110 module from *Toptica*

5.2.2 Results

D2 laser

The goal of this experiment is to determine the frequency of the atomic transitions, relative to the ULE, necessary for the laser cooling of lithium. Since the absolute frequency calibration of individual wave meters may differ, the frequency value of the specific wavemeter used in the lab must be determined. To this end, the frequencies at which the dips in the absorption spectrum occur can be calculated. This is done for both lasers.

The data measurements of the Doppler-free spectroscopy conducted with the D2 laser are plotted in Figure 24 and Figure 25.

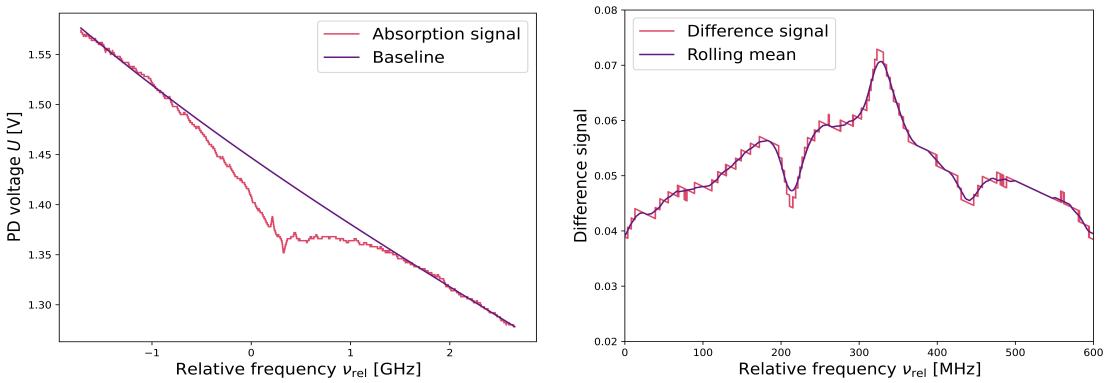

Fig. 24: The left plot shows the absorption line of the saturation spectroscopy performed with the D2 laser. The baseline is a fit that represents the laser light without interaction with the atomic cloud. Here, the peaks and dips can already be seen. The measured data of how much light the atoms absorb is shown on the right. Two Lamb dips and a cross-over peak can be observed, since two transitions with a common excited state are driven by the laser. In the figure the rolling mean from the difference signal has been plotted to see the curve more clearly and for better finding of the frequency of the peaks and dips.

The plot on the left image in Figure 24 shows the absorption line of the laser when interacting with the atoms, represented as the red line. The fitted purple curve shows the baseline of the laser without interacting with the atoms. The large sink is still visible, but additional dips and peaks can be seen in the middle of the lowering. These are caused by the transitions corresponding to the hyperfine structure. The light absorbed by the atoms is shown in the right plot of Figure 24. The frequency range is smaller such that the curve has higher resolution. Here the predicted Lamb dips that arise because of the two transition driven by the D2

laser are noticeable. By performing the same experiment and recording only the data where the peaks and dips are, a better resolution is obtained. This can be seen in Figure 25.

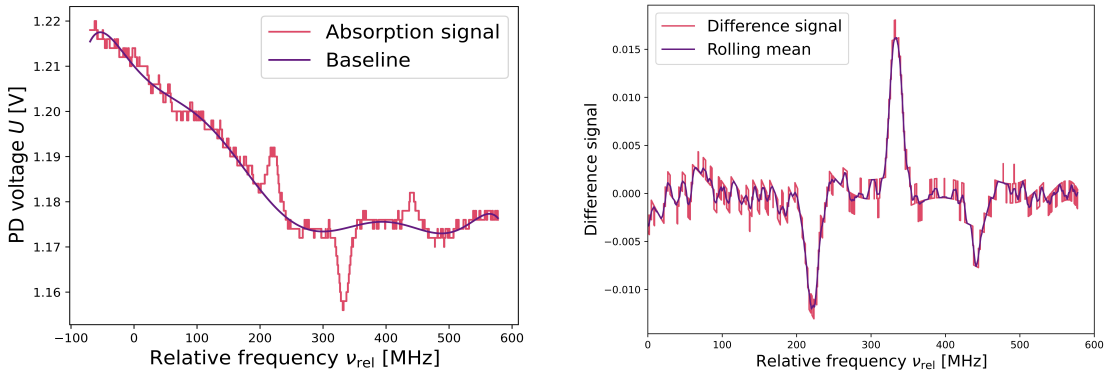

Fig. 25: The left plot shows the absorption line in red. The purple line shows the calculated absorption line if the laser would not interact with the atoms. The right plot shows the difference signal, representing how much light the atoms absorbed from the laser. Here the two Lamb dips and the one cross-over peak can be observed. In the figure the rolling mean from the difference signal has been plotted to see the curve more clearly and for better finding of the frequency of the peaks and dips.

In Figure 25 the peaks and dips of absorption spectrum are more clear. With this data the exact frequency of the transitions, relative to the ULE can be estimated. In the plots in Figure 25 the lamb dips are at 216 and 441 MHz, respectively, and the cross-over peak is at 331 MHz. The left Lamb dip is produced by the transition of the atoms from the upper ground state $2^2S_{3/2}$ to the excited state $2^2P_{3/2}$. The right lamb dip represents the absorption of light by the transition from the lower ground state $2^2S_{1/2}$ to the excited state $2^2P_{3/2}$. The three hyperfine levels of the excited state are only 4.4 MHz apart, so they appear as one common level as even the linewidth is wider (see Table 2). The exact value of the hyperfine-split between the $2^2S_{1/2}$ F = 3/2 and the $2^2S_{1/2}$ F = 1/2 is 228.2 MHz [13]. The value extracted from the plots in Figure 25 is 224 MHz. The 4 MHz deviation from the theoretical value is smaller than the linewidth of the states. The zero of the relative frequency scale corresponds to a frequency range of 446.7989 to 446.7994 THz, or from 670.979 nm to 670.978 nm, on the wavemeter. This values are needed to find the ULE peak that is the closest to the transition frequencies for laser cooling of lithium.

D1 laser

The measurements of the saturation spectroscopy conducted with the D1 laser on

lithium are shown in Figure 26.

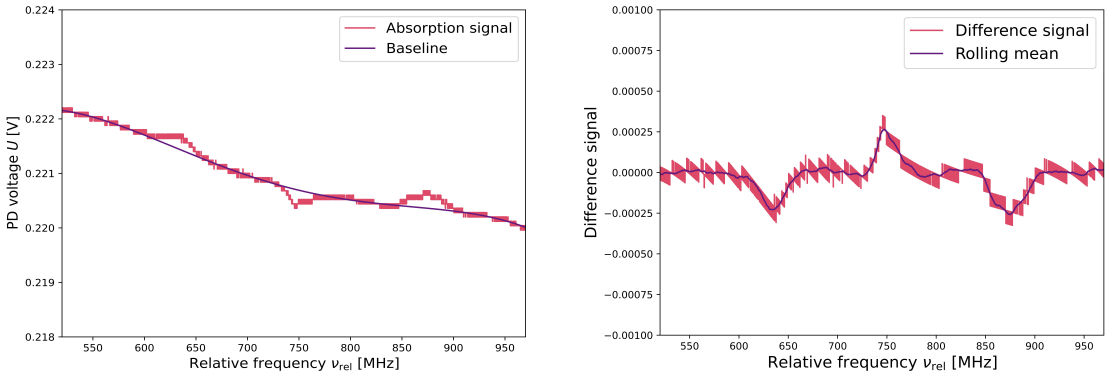

Fig. 26: The left plot shows the absorption line of the saturation spectroscopy performed with the D1 laser. The baseline represents the laser light without interaction with the atomic cloud. Here, the peaks and dips can already be seen. How much light the atoms absorb is shown on the right, as the difference signal. Two Lamb dips and a cross-over peak can be observed, since two transitions with a common excited state are driven by the laser. In the figure the rolling mean from the difference signal has been plotted to see the curve more clearly and for better finding of the frequency of the peaks and dips.

The predicted Lamb dips and cross-over can clearly be seen in Figure 26. There are to Lamb dips corresponding the two transition driven by the D1 laser to the excited $2^2P_{1/2}$ state from the upper ground state $2^2S_{3/2}$ and from the lower ground state $2^2S_{1/2}$. As the hyperfine-split energy levels of the excited state are only 26.1 MHz apart, they appear as one energy level in this spectroscopy measurements. That is why lithium can be represented as an effective three-level atom with two ground states and one excited state.

For the D1 laser the left dip seen in Figure 26 is at a frequency of 637 MHz and the right at 877 MHz, relative to the ULE peak. The cross-over peak is found at 745 MHz. With these values the distance between the lamb dips is calculated to 239 MHz. The theoretical frequency value between both lamb dips is 228 MHz [13]. This difference of 11 MHz comes from the uncertainty of the ULE peaks finder program. For improving the resolution the higher order peaks of the ULE can also be used as a reference, and as they are not so far apart, better results can be achieved. This has been done for the D2 laser.

6 Laser Locking

The focus of this work is to build a laser system to drive atomic transitions in lithium. These transitions have very specific wavelengths. Since they are driven by lasers, they must have the same specific frequency. However, changes in the environmental condition - such as temperature or pressure fluctuations in the lab - can lead to drifts in the laser frequency, which eventually result in mode hops. To stabilize the system, the lasers must be locked to a wavelength. For this prupose laser locking techniques have been developed, the one used here is a Pound-Drever-Hall (PDH) lock. This method is used to lock the frequency of a laser to the resonance frequency of an optical cavity.

6.1 D1 and D2 Laser Lock with Pound-Drever-Hall Technique

In this experiment, the PDH technique is used to lock the two lasers, for the D1 and the D2 line. The optical cavity used for this is the previous mentioned ULE. The main idea of this locking method is to create an error signal that is not symmetric around the zero crossing, such that therefore if the lasers drift, its drift-direction is known and a PID can counteract the shift. The main components required are a phase modulator or electro-optical modulator (EOM), an optical cavity, a mixer and a low-pass filter, and a PID controller. The EOM modulates the phase of the laser beam, creating sidebands around the center-frequency of the main peaks obtained from the ULE. These sidebands are necessary to create a correct PDH error signal. The sidebands signal is mixed with the reflected light and gets measured with a photodiode. After processing, the error signal is generated with the Pound Drever Hall detector module from "Toptica". This error signal is fed to the PID controller[5] so that it can correct the drifts of the laser.

6.1.1 Setup

To lock the lasers, the same setups as for the spectroscopy measurements was used, which can be seen in Figure 23. For the ULE the setup represented in Figure 18 and for the D1 also the setup in Figure 26 was utilized. The rest of the elements needed such as the RF oscillator, the phase shifter and the mixer are integrated

[5]FALC110 Module from *Toptica*

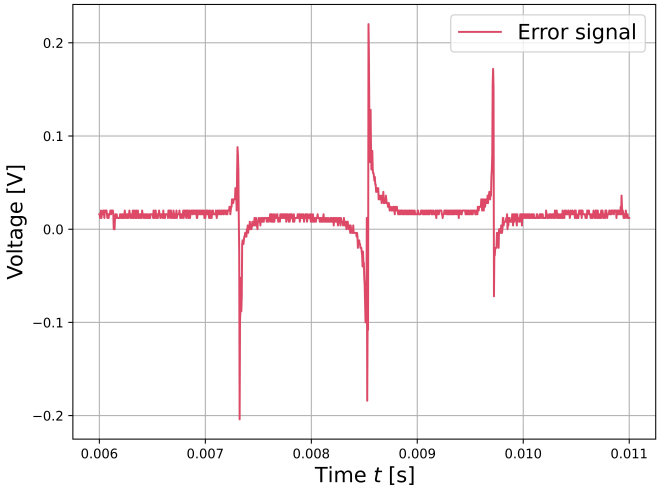

Fig. 27: Pound Drever Hall error signal for the lock of the D2 laser.

in the modul[6]. The PID is also integrated in a module[7]. To lock the lasers the reflected ULE signal is recorded at a photodiode and fed to the aforementioned PDH module, which then creates the error signal. For creating the side bands on the laser frequency a fiber EOM[8] is used.

The sidebands are ± 25 MHz apart from the lasers frequency and are created by an internal RF oscillator in the Pound Drever Hall module. As described in equation Equation 3.12, the reflected signal contains multiple terms oscillating at different frequencies of which only one is of interest for the error signal. This can be achieved with a low pass filter. For this, the signal of the photodiode gets combined with a sinusoidal signal in order to eliminate all the non constant terms. When this signal passes through the low pass, only one constant term can get through. This term is the error signal.

After performing the laser lock with the D1 and D2 lasers, the error signal shown in Figure 27 could be seen. Also the compensation of the laser drift by the FALC 110 module could be observed at the oscilloscope.

[6]Pound-Drever-Hall Detector module
[7]FALC 110 module from *Toptica*
[8]Phase modulator from *JENOPTIK*

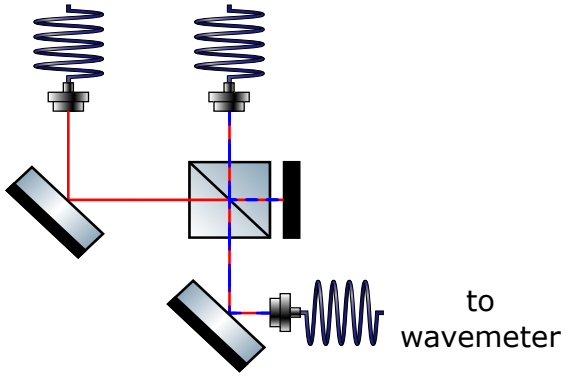

Fig. 28: Schematic representation of the setup used for the stability measurement. The D1 or D2 laser, respectively for each stability measurement, were connected to the most left fiber, and the transition locked 780 nm laser into the right fiber. This second laser was used to record the drift of the wavemeter

6.2 Long Term Stability of the Lasers

After locking both lasers, the stability of the lock was examined. This is done by performing a long-term stability measurement. In this experiment, the stability of the wavelength of the laser is recorded over a long period of time (e.g. over an hour) to see if it remains stable. The setup used for the measurement can be seen in Figure 28.

This measurement was performed on both lasers and can be seen in the left plot of Figure 29 for the D1 laser and on the right plot in the same figure for the D2 laser.

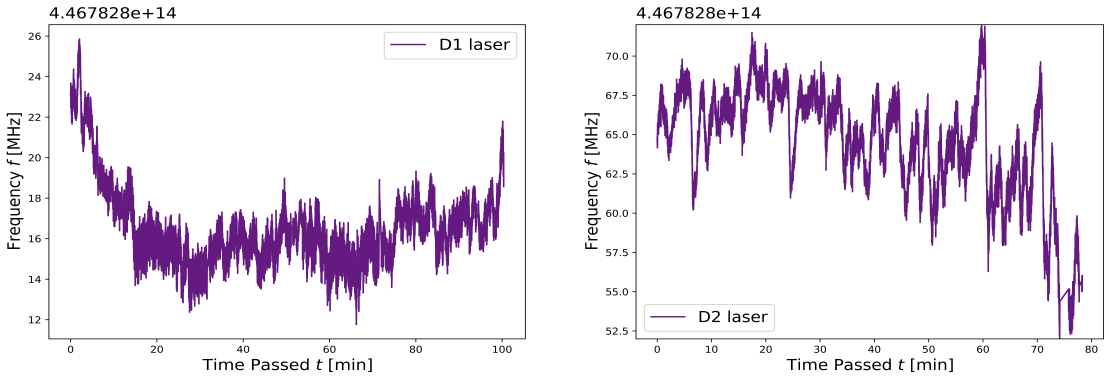

Fig. 29: Long term stability measurement of the D1 laser on the left and of the D2 laser on the right.

A possible drift and jitter of the wavemeter frequency was also measured by monitoring the wavemeter with a transition locked 780 nm laser. The wavemeter drifted short term by about ± 3 MHz. The overall measured drift of the locked lasers was on the order of 10 MHz for both the D1 and the D2 lasers. Taking into account that the linewidth of the energy states is 6 MHz (see Table 2) and the aforementioned drift of the wavemeter itself, it can be said that the lock works sufficiently well and the lasers are ready to be used for the laser cooling.

7 Summary and Outlook

This thesis reports on the setup, characterization and improvement of a laser system for the cooling of lithium via gray molasses. A second laser used for the MOT and for the Zeeman slower is also investigated in order to perform lithium spectroscopy and frequency stabilization.

The laser used for the gray molasses drives the D1 transition of lithium and the one used for the Zeeman slower excites the D2 transition. To characterize and improve the D1 laser, its inner characteristics such as the power and the wavelength dependence on various factors were investigated. After that, the beam shape was improved with two anamorphic prism pairs in order to make it more Gaussian shaped. This allows for a better coupling efficiency in single mode fibers, which are used later in the experiment.

Second, the exact wavelength of the lithium transitions was investigated via Doppler-free spectroscopy. The D1 transitions were found at 637 and 877 MHz with respect to the nearest ULE peak and the D2 transition were observed at 216 and 441 MHz in the relative frequency scale. These wavelengths are the ones at which the lasers have to be run for the main experiment. To be sure that the lasers remain at these wavelengths, the Pound Drever Hall locking method is used. Both lasers could be locked for over an hour with negligible perturbations as it can be seen in Figure 29.

For further improvement of the setup, the D1 laser will be phase locked to the D2 laser, which will still be locked with the Pound Drever Hall method. The phase locking technique allows to use an already stabilized laser, such as the D2, to lock a second laser, if both lasers are close to each other in frequency. In this case both lasers are only 10 GHz apart allowing the usage of this technique. This is done to allow the lock of other lasers with the PDH technique to the ULE, avoiding overlapping in the cavity.

The main application of the D1 laser is to be used for gray molasses cooling of lithium. This is a secondary cooling technique after the trapping of lithium atoms by a MOT to achieve temperatures where the s-wave scattering regime becomes approachable. For this, the laser light has to be implemented in the ion microscope experiment. After the laser is locked to the nearest ULE peak, its wavelength needs to be shifted to the actual transition. This can be done with Acusto-Optical Modulators (AOMs), which will also be implemented in the main experiment.

When the D1 and D2 lasers and all extra optical elements are implemented in the ion microscope, the cooling and trapping of lithium will be possible, which will enable the realisation of experiments such as the scattering between ions and ground states atoms. In addition, the creation and investigation of a lithium Fermi-sea will be possible. The ion microscope can then also be used to investigate lithium-rubidium mixtures, which will permit the study of the interactions between both atomic species.

8 Appendix

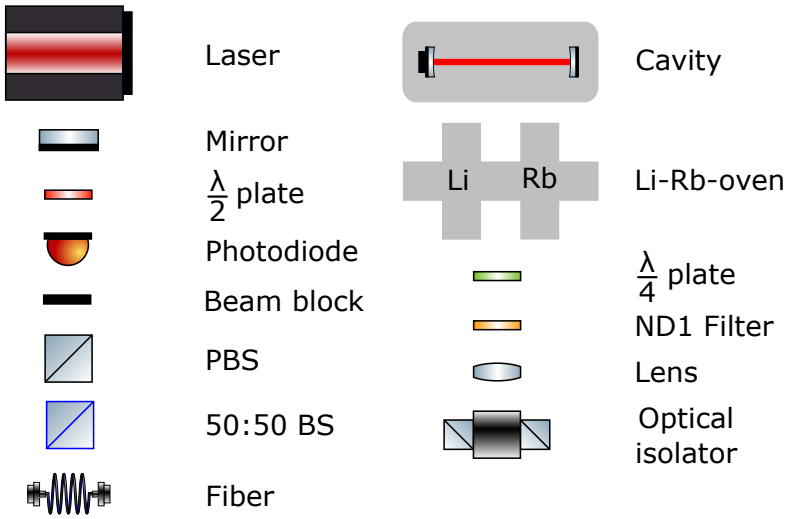

Fig. 30: Legend of the optical elements used in the setup representations.

9 References

[1] Waseem S Bakr, Jonathon I Gillen, Amy Peng, Simon Fölling, and Markus Greiner. "A quantum gas microscope for detecting single atoms in a Hubbard-regime optical lattice". In: *Nature* 462.7269 (2009), pp. 74–77.

[2] Jacob F Sherson, Christof Weitenberg, Manuel Endres, Marc Cheneau, Immanuel Bloch, and Stefan Kuhr. "Single-atom-resolved fluorescence imaging of an atomic Mott insulator". In: *Nature* 467.7311 (2010), pp. 68–72.

[3] Markus Stecker, Hannah Schefzyk, József Fortágh, and Andreas Günther. "A high resolution ion microscope for cold atoms". In: *New Journal of Physics* 19.4 (2017), p. 043020.

[4] Zbigniew Idziaszek, Tommaso Calarco, Paul S Julienne, and Andrea Simoni. "Quantum theory of ultracold atom-ion collisions". In: *Physical Review A—Atomic, Molecular, and Optical Physics* 79.1 (2009), p. 010702.

[5] T Schmid, C Veit, N Zuber, R Löw, T Pfau, M Tarana, and M Tomza. "Rydberg molecules for ion-atom scattering in the ultracold regime". In: *Physical review letters* 120.15 (2018), p. 153401.

[6] Christian Veit. "An ion microscope to probe quantum gases on the single-atom level". PhD thesis. Stuttgart: Universität Stuttgart, 2021.

[7] Yi-Quan Zou, Moritz Berngruber, Viraatt SV Anasuri, Nicolas Zuber, Florian Meinert, Robert Löw, and Tilman Pfau. "Observation of vibrational dynamics of orientated Rydberg-atom-ion molecules". In: *Physical Review Letters* 130.2 (2023), p. 023002.

[8] Moritz Berngruber et al. "*Insitu* observation of non-polar to strongly polar atom-ion collision dynamics". In: *arXiv preprint arXiv:2401.12312* (2024).

[9] Ruven Simon Conrad. "Design and setup of a Rb-Li dual-species vapor source for an ultracold atoms experiment". Master Thesis. University of Hamburg, 2023.

[10] C Veit, N Zuber, OA Herrera-Sancho, VSV Anasuri, T Schmid, F Meinert, R Löw, and T Pfau. "Pulsed ion microscope to probe quantum gases". In: *Physical Review X* 11.1 (2021), p. 011036.

[11] Nicolas Zuber, Viraatt SV Anasuri, Moritz Berngruber, Yi-Quan Zou, Florian Meinert, Robert Löw, and Tilman Pfau. "Observation of a molecular bond between ions and Rydberg atoms". In: *Nature* 605.7910 (2022), pp. 453–456.

[12] J Joger, H Fürst, N Ewald, T Feldker, Michał Tomza, and R Gerritsma. "Observation of collisions between cold Li atoms and Yb+ ions". In: *Physical Review A* 96.3 (2017), p. 030703.

[13] Michael E. Gehm. *Properties of Lithium*. Last accessed: 2023-07-14. URL: https://jet.physics.ncsu.edu/techdocs/pdf/PropertiesOfLi_2016.pdf.

[14] Thorlabs. *Advantages and disadvantages of diode lasers*. Last accessed: 2023-07-06. URL: https://www.toptica.com/technology/technical-tutorials/tapered-amplifiers#gallery.

[15] Thorlabs. *Achievable Wavelenghts with diode lasers*. Last accessed: 2023-07-06. URL: https://www.thorlabs.com/navigation.cfm?guide_id=2164.

[16] Laser Focus World. *Diode Laser characteristics*. Last accessed: 2023-07-14. URL: https://www.laserfocusworld.com/lasers-sources/article/16556280/diode-lasers-research-gives-high-power-diode-lasers-new-capabilities.

[17] Wikipedia. *Advantages and disadvantages of diode lasers*. Last accessed: 2023-07-06. URL: https://de.wikipedia.org/wiki/Diodenlaser#:~:text=Optische%20Ausgangsleistung%3A%20bis%2090%20W,von%20808%20bis%20980%20nm.

[18] Britannica. *Spectroscopy*. Last accessed: 2023-07-07. URL: https://www-britannica-com.translate.goog/science/spectroscopy.

[19] Wikipedia. *Doppler Shift*. Last accessed: 2023-07-14. URL: https://de.wikipedia.org/wiki/Dopplerverbreiterung.

[20] Christopher J. Foot. *Atomic Physics*. Oxford University Press 2005, 2005. ISBN: 978-0-19-85069-6.

[21] Sana Pyka Aline Dinkelaker Marek Mandel. *Laser spectroscopy with rubidium*. Last accessed: 2023-07-23. URL: https://www.physik.hu-berlin.de/en/qom/lehre/f-praktikum-laserspektroskopie/anleitung.pdf.

[22] Josephine Gutekunst. "EIT Spectroscopy in Hollow Core Fibers". Bachelor Thesis. University of Stuttgart, 2016.

[23] Wikipedia. *Absoprtion Cross-section*. Last accessed: 2023-07-14. URL: https://en.wikipedia.org/wiki/Absorption_cross_section.

[24] Zurich Instruments. *Principles of PID Controllers*. Last accessed: 2023-07-15. URL: https://www.zhinst.com/europe/en/resources/principles-of-pid-controllers.

[25] Eric D. Black. *An introduction to Pound–Drever–Hall laser frequency stabilization*. Last accessed: 2023-07-15. URL: https://edisciplinas.usp.br/pluginfile.php/5095949/mod_resource/content/1/Pound-Drever-Hall_Introduction__AJP.pdf.

[26] HAL open science. *Ultracompact reference ultralow expansion glass cavity*. Last accessed: 2023-07-16. URL: https://hal.science/hal-02138795/document.

[27] Einius Pultinevicius. "A laser frequency stabilization scheme for the cooling of barium monofluoride molecules". Master Thesis. University of Stuttgart, 2022.

[28] Wikipedia. *Second-harmonic generation*. Last accessed: 2023-07-17. URL: https://en.wikipedia.org/wiki/Second-harmonic_generation.

[29] Dr. Rüdiger Paschotta. *Free Spectral Range*. Last accessed: 2023-07-19. URL: https://www.rp-photonics.com/free_spectral_range.html.

[30] Daniel Halwidl and Daniel Halwidl. "Effusive molecular beam sources". In: *Development of an Effusive Molecular Beam Apparatus* (2016), pp. 19–23.

[31] Christian Thomschitz. "Aufbau eines Diodenlasers zur hochauflösenden Spektroskopie von Lithium". Bachelor's Thesis. University of Stuttgart, 2016.

Acknowledgements

I would like to thank everyone who has supported me in this work. I would like to thank in first place DR.PROF. TILMAN PFAU for giving me the opportunity to write my Bachelor's thesis at the 5th Institute of Physics. Dr. ROBERT LÖW for always having a solution for the arising problems during this work. Of course, the Ryblis: ÓSCAR HERRERA, MORITZ BERNGRUBER, JENNIFER KRAUTER, RUVEN CONRAD, RAPAHEL BENZ and my supervisor OLE PROCHNOW. I had an amazing time working with you, thank you for making physics so interesting, for your help and for always having time to help me. Also to all the other members of the institute which I could also meet and have good time with. Als nächstes würde ich gerne meine Komilitonen während des studiums danken, mit speziall mention an MICHELLE WEISS, mit der ich neben der Physik ganz viele andere Erlebnisse leben konnte. An meine deutsche Familie, die mir stets bei Seite stand, und mich motiviert hat in Deutschland zu studieren. També he de fer especial menció a tota la familia valenciana, els del present i els del passat, que sempre m'han rebut en els brassos oberts, m'han ajudat en tot el que han pogut i han fet de cada situació una millor. Als meus amics, en els que he pogut créixer i disfrutar durant tants anys, en especial menció a GERARD, per sempre haver estat.
ERIC danke ich für die essenzielle Begleitung in den letzten Jahren, die zu einem sehr grossen Teil dazu beigetragen haben mir einen neues Leben in Deutschland aufzubauen. Per a acabar, donar les gràcies a els meus pares, INÉS I OLIVER, i a la meua germana, AISHA, que m'han recolzat en tot moment i han fet possible que acabara esta carrera. Moltes gràcies.